KLEITON LIMA DE GODOY MACHADO

THE MODULE MIR156/SPL AFFECTS BIXIN BIOSYNTHESIS PATHWAY IN ANNATTO (*Bixa orellana* L.).

Thesis submitted to the Plant Physiology Graduate Program of the Universidade Federal de Viçosa in partial fulfillment of the requirements for the degree of *Doctor Scientiae.*

Adviser: Wagner Campos Otoni

Co-adviser: Daniele Vidal Faria

VIÇOSA - MINAS GERAIS
2022

Ficha catalográfica elaborada pela Biblioteca Central da Universidade Federal de Viçosa - Campus Viçosa

T

M149m
2022

Machado, Kleiton Lima de Godoy, 1990-
The module mir156/spl affects bixin biosynthesis pathway in annatto (*Bixa orellana* L.). / Kleiton Lima de Godoy Machado. - Viçosa, MG, 2022.
1 tese eletrônica (80 f.): il. (algumas color.).

Texto em inglês
.

Orientador: Wagner Campos Otoni.
Tese (doutorado) - Universidade Federal de Viçosa, Departamento de Biologia Vegetal, 2022.
Referências bibliográficas: f. 64-80.
DOI: https://doi.org/10.47328/ufvbbt.2022.323
Modo de acesso: World Wide Web.

1. Fenologia vegetal. 2. Urucum. 3. *Bixa orellana*. 4. Metabólitos. 5. Proteínas - Metabolismo. I. Otoni, Wagner Campos, 1962-. II. Universidade Federal de Viçosa. Departamento de Biologia Vegetal. Programa de Pós-Graduação em Fisiologia Vegetal. III. Título.

CDD 22. ed. 578.42

Bibliotecário(a) responsável: Euzebio Luiz Pinto CRB 6/3317

KLEITON LIMA DE GODOY MACHADO

THE MODULE MIR156/SPL AFFECTS BIXIN BIOSYNTHESIS PATHWAY IN ANNATTO (*Bixa orellana* L.).

Thesis submitted to the Plant Physiology Graduate Program of the Universidade Federal de Viçosa in partial fulfillment of the requirements for the degree of *Doctor Scientiae.*

APPROVED: April 4, 2022

Assent:

Kleiton Lima de Godoy Machado
Author

Wagner Campos Otoni
Adviser

ACKNOWLEDGEMENTS

First, I would like to express my gratitude to all Brazilians who paid taxes and supported the excellence of public schools. From farmers to lawyers, men and women, who shed blood, sweat, and tears across Brazil's history and nowadays, you all made this research possible. So, thank you!

To my adviser, professor Wagner Campos Otoni, who has been responsible to enlighten my career, showing that it is possible to be a great scientist and an extraordinary human being. You rescued my dreams, and for this, I will be grateful forever.

My steps would never be possible without the unconditional support of my family; thank to my mom, Marília, for not giving up on my dreams even if it had cost you a lot. My dad, Julio Cesar, for always having a support message and teaching. Also, thanks to my grandparents, Eda, for raising me as her child and showing me that love is about taking care of each other. Vera, for showing me even in the darkest hour we will strive. Edenir, my grandpa, for you to have lit up my scientific thinking since my early days. Thanks to my brother Juliano and my sister Graziella, I am doing this for you. To my stepfather and stepmother, Flávio and Dalva, thank you for showing me love and care, and for inviting me into your lives. All these achievements are consequences of your efforts!

For making my life bright and hopeful, my companion, friend, and lover: Letícia, thank you to being supportive even in moments when you needed it the most. You have shown me that my dreams were feasible and, with you, I can reach everything.

Thanks to my first advisers: Eliane Santarem and Leandro Astarita, you have taught me with patience and love since my early days in the lab. As well, my labmates from Biotecnologia Vegetal, thank you!

I have to thank my cousins, aunts, and uncles for making me feel loved and for always being proud of me. I would like to express my honest love and gratitude to my dearest brothers Eugênio Araújo, Matheus, and Thomas Vieira, your brotherhood has always been my foundation to achieve everything. Also, their parents: Lígia and João Vieira, always take care of me as one of their children. Thank you!

My thanks would not be enough to all my friends from Rio Grande do Sul, in special to Wagner Fagundes, Rafaela Nozari, Francielli Ortolan, Daniele Figueiró,

Kimberly Marta, Géssica Antunes, Luiza Funez, Carolina Luft, Anderson Catarina, Guilherme Oliveira and Thomas Dias. You have supported me with examples of intelligence and talent. Besides, my greatest joy is to know that you are taking care of my back always.

Starting a new life was not easy and without the support of numerous people that I met in Viçosa, my achievements would not be possible: Rodrigo, who showed me how things work here and helped in my scientific and personal maturity. Alefe, always supported me, even when things were not good for you. Dalton, for being my older brother and for always taking care of me. Lucas Cavalcante, for the many great talks and exhaustively bad jokes. Webert, for showing me compassion and brotherhood. Maurino, for showing how a human being can be amorous and concerned about the well-being of others. Sabrina Araujo, for the best English classes ever and a little bit of psychological support. Michel, for the teachings and reflections. Eduardo and Carlos for being my wingmen in projects and absolutely every crazy idea I came up with. Diego, Matheus, and Ueslei, for standing beside me every day, showing me love and compassion. To my “pelada” mates: Auderlan, Renato, Bruno, Gustavo, Nain, Marco Antonio, Carlos Aucique, Daniel Oliveira, Adans, Angel, Wellington, Pedro, Leonardo, Daniel Coelho Christian Grabowsky, and Christian Zuluaga. Thanks for making my life easier and brighter.

I am in an awesome research group and I am thankful for that: To my co-adviser, Dr. Daniela Faria, thank you for being patient and supportive with your great ideas and hard work. Professor Diego Batista: thank you for teaching me every protocol with patience and wiliness. To professors Dimas Ribeiro and Fabio Nogueira, for the teachings and for helping me with smart correlations and reflections. To professors Vanildo Silveira and Claudete Santa-Catarina, Dr. Tadeu dos Reis de Oliveira, and Dr. Vinicius de Souza for helping me in proteomic analysis with patience and rapid response.

To all my colleagues, Evandro, Jéssica, Jessenia, Lorena, Marcos Dutra, Marcos Barbosa, Tatiane, Quézia, Pedro, José Victor, Kamila, Márcia, Ana, Paloma, Raíssa, Evandro, Lázara, Elizandra, Gabriel, Edson and Victor, and all the Palma group, who helped me every time they could; you made my path joyful every day.

In addition, I want to thank my colleagues from Fisiologia Vegetal and the UFV staff: Professor Fabio DaMatta, Professor Samuel Martins, Kelly Fonseca, “Lili’,

Luciene, Reginaldo, Guilherme, Geraldo “Marreco”, “Toninho”, Maria Mercês, and “Seu Zé” for being helpful and supportive in most of my trajectory.

Finally, I want to thank UFV, CNPq (grant 146061/2019-5), CAPES (Finance Code 0001), and FAPEMIG (grants APQ-02372-17 and APQ-00772-19), for providing infrastructure and scholarship. This work would not be possible without you all.

“So the problem is not so much to see what nobody has yet seen, as to think what nobody has yet thought concerning that which everybody sees.”

(Arthur Schopenhauer)

ABSTRACT

MACHADO, Kleiton Lima de Godoy, D.Sc., Universidade Federal de Viçosa, April, 2022. **The module mir156/spl affects bixin biosynthesis pathway in annatto (*Bixa orellana* L.).** Adviser: Wagner Campos Otoni. Co-adviser: Daniele Vidal Faria.

Annatto [*Bixa orellana* L. (Bixaceae)] is a woody plant species that can reach up to 6 meters in height, with a fast growth pattern. Annatto produces a main apocaterotenoid namely bixin, a unique natural dye. This compound is highly used in the textile, pharmaceutical and food industries, among others, making annatto an important crop in both ecological and economic aspects. Despite its relevance, there are several gaps for the understanding of its developmental processes. Perhaps one of the most interesting is the role of miR156/SPL module in its physiology. This microRNA is responsible for integrating plant physiology development through modulation of SPL transcription factors that modulate leaf morphology and anatomy, among other characteristics that may be linked to secondary metabolites production. In this particular, the miR156/SPL module regulates the biosynthesis of sesquiterpenes, flavonoids, anthocyanins, and carotenoids in higher plants. In this context, *B. orellana* is a promising woody species with an expressive secondary metabolism activity. Therefore, we aimed to assess phenotypic changes, plant phenology, hormonal profile, secondary metabolism, expression of developmental-linked genes, and proteome portray in overexpressing miR156 lines of *B. orellana* plants (OE::156). We observed new patterns in plant architecture and leaf blade features. In addition, higher IAA and ABA levels were found in OE::156 plants compared to non-transformed plants (Nt). Moreover, OE::156 plants have lower bixin content than Nt. Furthermore, CCD4 showed lower expression in contrast to higher CCD1 transcriptional levels. Besides that, the proteome showed ZEP upaccumulation in OE::156 plants, which indicates that carbons are being translocated from bixin to ABA production. Further studies are suggested to understand the role of specific secondary metabolites regulation by miR156/SPL module.

Keywords: microRNA. SPL proteins. Plant development. Phase change. Proteomics.

RESUMO

MACHADO, Kleiton Lima de Godoy, D.Sc., Universidade Federal de Viçosa, abril de 2022. **The module mir156/spl affects bixin biosynthesis pathway in annatto (*Bixa orellana* L.).** Orientador: Wagner Campos Otoni. Coorientadora: Daniele Vidal Faria.

O urucum [*Bixa orellana* L. (Bixaceae)] é uma planta lenhosa de porte médio, com rápido padrão de crescimento. A espécie possui um metabolismo secundário relativamente ativo, onde o principal metabólito é um apocarotenoide denominado bixina, largamente utilizado nas indústrias têxtil, farmacêutica e alimentícia, entre outras, tornando o urucunzeiro uma cultura economicamente importante. A despeito de sua relevância, existem várias lacunas sobre seus processos de desenvolvimento. Talvez um dos mais interessantes seja o papel do módulo miR156/SPL em seu desenvolvimento e fisiologia, pois microRNA é responsável por integrar estes dois processos através da regulação de fatores de transcrição SPL que modulam características morfoanatômicas. Ainda, o módulo miR156/SPL regula a biossíntese de compostos secundários como sesquiterpenos, flavonoides, antocianinas e carotenoides em plantas superiores. Portanto, o objetivo desse trabalho foi avaliar alterações fenotípicas, fenologia vegetal, perfil hormonal, metabolismo secundário, expressão gênica ligada ao desenvolvimento e perfil do proteoma em linhagens de plantas de *B. orellana* superexpressando miR156 (OE::156). Com isso, observamos novos padrões na arquitetura das plantas e nas características das lâminas foliares. Além disso, também descobrimos níveis mais altos de AIA e ABA em plantas OE::156. Ademais, descobrimos que plantas OE::156 apresentam menor teor de bixina do que plantas não transformadas (Nt). Além do mais, observamos que CCD4 apresentou menor expressão em níveis transcricionais a destarte de níveis mais altos de transcritos de CCD1. Além disso, o proteoma apresentou acúmulo de proteínas ZEP em plantas OE::156, o que indica que os carbonos estão sendo translocados da produção de bixina para biossíntese do fitormônio ABA. Em adição aos resultados apresentados, sugere-se mais estudos para expandir o endentimento do papel do módulo miR156/SPL na regulação de metabólitos secundários específicos na espécie-alvo.

Palavras-chave: microRNA. Proteínas SPL. Desenvolvimento vegetal. Troca de fase. Proteoma.

SUMMARY

1. INTRODUCTION

1.1 *Bixa orellana*: importance and potential

Popularly known as Annatto, *Bixa orellana* L. (Bixaceae) belongs to the order Malvales, with important representatives such as Cocoa, Hibiscus, and Cotton (The Angiosperm Phylogeny Group II 2003; The Angiosperm Phylogeny Group III 2009). Although planted around the world, annatto was domesticated from *B. urucurana* by the southern Amazonia native people, long before the European invasions of South America (Moreira et al. 2015). Since the European raids, the western world has used this plant as the only source of the apocarotenoid bixin, since 80% of all pigments present in *B. orellana* is bixin. (Oliveira et al. 1996; Ramamoorthy et al. 2010). In addition, several emerging countries such as Angola, India, and Brazil have planted and exploited this culture as a commodity. (https://www.cabi.org/isc/datasheet/9242#C19AC032-9D96-488E-BE68 7972662568B4). Also, the World Health Organization (WHO) pointed to bixin as one of the few non-toxic dyes, as it is taken from a natural source, does not change the nutritional factors of foods, and has wide use in Brazil, in the form of *colorau* (Bastos et al. 1999; Vilar et al. 2014). Furthermore, annatto has one of the few natural hydrophilic dyes, norbixin. (Giuliano et al. 2003; Rivera-Madrid et al. 2013). As a result, bixin and norbixin are very important for the pharmaceutical, cosmetic, and textile industries worldwide. (Valério et al. 2015).

Annatto is a woody plant, native to the Neotropics. This shrub can reach up to 6 meters in height, with heart-shaped dotted or serrated leaves, hermaphrodite flowers with 5 blue-pink petals with 2 to 3 carpels, from which the ovoid capsules originate. Flexible spines cover the capsules, and the fruit has an average of 54 seeds with a reddish integument (Baliane 1982). This species has a rapid growth pattern, reaching the reproductive age after 18 months of germination (De Góes 1998). However, these plants do not show an apparent change of vegetative phases (from juvenile to adult) like other woody plants such as *Eucalyptus globulus* (Lucani et al. 2019), *Acacia koa* (Rose et al. 2019), and *Vachellia collinsii* (Leichty and Poethig 2019). *B. orellana* has extrafloral nectaries in its stem and in the floral receptacles that exude and offers sugar,

attracting ants that will defend the plants from possible herbivore attacks (Bentley 1977; Miranda et al. 2017). Additionally, its seeds have a high content of carotenoids that are stored in their cells with high numbers of chromoplasts and dense globules that fused with the vacuole (Louro and Santiago 2015). Besides, annatto has broad-spectrum antimicrobial action (Karmakar et al. 2018), because it produces several compounds such as terpenes, sesquiterpenes, alkaloids, among others, as reviewed in Santos et al. (2021).

Along with its economic and cultural aspects, this woody shrub is a potential model for studies of development and secondary metabolism modulation, as annatto has rapid growth, flowering, and fruit settling. Further, annatto has a high carbon demand for bixin biosynthesis, a metabolite biogenesis route that is highly active when compared to other woody species. Additionally, apart from the high levels of bixin, constitutively produced in annatto, it also has other secondary compounds. Still, studies with this species can shed light and expand the understanding of how molecular hubs, such as the miR156/SPLs module, acts in the regulation of vegetative phase change (from juvenile to adult) and different types of metabolites production in woody plants.

1.2 The miR156/SPL module role in plants

Non-coding RNAs are crucial in the gene expression regulation linked to development in eukaryotes. These molecules have approximately 22 nucleotides that are capable of pairing in the 3' UTR (untranslated region) or even in the target mRNAs ORFs (open reading frames), forming secondary structures that will repress translation. In plants, these molecules were described by Llave et al. (2002) and their assigned functions, as part of plant development regulation by Reinhart et al. (2002). Transcription of primary microRNA (pri-miRNA) is the first step in miRNA biogenesis. Thereafter, this pri-miRNA is recognized by the enzyme DICER-LIKE 1, which cleaves the pri-miRNA into two miRNAs, producing a duplex that is exported by a process involving exportin proteins HASTY and TREX-2 to the cytoplasm (Bollman et al. 2003; Kurihara and Watanabe 2004; Park et al. 2005; Fahlgren et al. 2007; Bologna et al. 2018; Zhang et al. 2020). In the cytoplasm, the ARGONAUTE protein, which belongs

to the RISC (RNA-Induced Silencing Complex), recognizes the duplex. Then, the duplex is separated and RISC stabilizes and directs the single-stranded miRNA to the repression target (Kurihara e Watanabe 2004; Baumberger and Baulcombe 2005; Pratt and MacRae 2009; Liu et al. 2018).

MiRNAs play a central role in various plant development programs as they are responsible for the regulation of transcriptional factors involving cell division, organ differentiation, nutrition, and phenological transition in plants (Jones-Rhoades et al. 2006; Johnson et al. 2017). One of the most interesting processes coordinated by these molecules is the transition from juvenile to adult state, during the vegetative growth, orchestrated by the miR156-SPL module. This regulatory network appears to have originated very early in the evolutionary history of plants, as it is conserved in most angiosperms (Wu and Poethig 2006; Poethig 2009; Fouracre and Poethig 2019; Zheng et al. 2019).

The Squamosa Promoter-Binding Protein-Like (SPL) family of transcription factors encompasses genes related to phase switching in most plants. Furthermore, from 17 SPL genes discovered in plants, 11 are regulated by miR156 (Cardon et al. 1999; Wang et al. 2009; Wu et al. 2009; Yu et al. 2010). Therefore, the SPL family is largely regulated by miR156 in *Oryza sativa* (Xie et al. 2012)*, Nicotiana tabacum* (Feng et al. 2016)*, Pyrus pyrifolia* (Qian et al. 2017), *Arabidopsis thaliana* (Wu e Poethig 2006; Zheng et al. 2019), *Passiflora edulis* (Silva et al. 2019), and *Populus tremula* (Lawrence et al. 2021). This comprehensive regulation within plants is responsible for changes in leaf morphology and anatomy, trichome formation, male fertility (anther development), phytomer length and composition, glucose and trehalose metabolism, among other characteristics that may be linked to environmental factors as well (Wang et al. 2009; Xing et al. 2010; Yu et al. 2010; Poethig 2013; Fouracre and Poethig 2016; Silva et al. 2019; Lawrence et al. 2020b).

Specific studies have shown correlations between miR156/ SPL module and abiotic and biotic stresses. Plants that overexpress miR156 tend to be more tolerant to salt and water stress, as demonstrated by Cui et al. (2014), where Arabidopsis plants delayed their flowering and were able to tolerate such adverse events. The same phenomenon was observed in alfalfa and even in halophytic plants (Feyissa et al. 2019; Wang et al. 2019a). Also, jasmonic acid, which is a phytohormone related to the response against herbivory in plants, had higher levels during the adult phase and,

contrary to expectations, had lower responses in plants overexpressing miR156. This metabolic pattern is a result of the SPL9 interaction with the Jasmonate-zim domain (JAZ) proteins, stabilizing them. As a result, the plants developed the ability to attenuate responses to jasmonate but were able to proceed with high levels of defense compounds (Mao et al. 2017). With this example of how the miR156/SPL module interacts with phytohormonal responses, some authors have observed other processes related to hormonal signaling such as embryogenesis in Citrus callus, which is a process mediated by auxins and cytokinins (Long et al. 2018); development of lateral roots through signal transduction involving auxins (Yu et al. 2015a); stomatal closure during drought stress via strigolactones (Visentin et al. 2020); attenuation in root meristems of primary roots via cytokinins, promoting differentiation and thus new roots (Barrera-Rojas et al. 2020).

In addition to these aspects, the miR156/SPL module regulates the biosynthesis of secondary compounds during plant growth and development. Even if the increase or decrease of such compounds production is responsive under different environmental conditions. For example, in Arabidopsis, sesquiterpene levels are affected by SPL9 and SPL10, both targets of miR156, through activation of the TPS21 gene (*terpene synthase* 21) (Yu et al. 2015b). This module also regulates the flavonoid biosynthesis process, where miR156 prevents the translation of SPL9, resulting in anthocyanin accumulation at the junction of the stem and leaves of *Arabidopsis* (Gou et al. 2011). Furthermore, miR156/SPL hub also regulates carotenoid biosynthesis. In another study, transgenic Arabidopsis plants overexpressing miR156 showed higher levels of carotenoids in their seeds, via regulation of the transcription factor SPL15 (Wei et al. 2012). Additionally, the SPL16 gene was shown to be responsible for the increase in carotenoids in banana (*Musa acuminata*) fruits (Zhu et al. 2020). Furthermore, the involvement of the miR156/SPL module in the biosynthesis of the secondary compound of woody plants was also reported in poplar plants overexpressing miR156 (Wang et al. 2020b). The authors observed higher levels of anthocyanins and flavonoids compared to non-transformed plants. Within this scenario, we hypothesized that, in addition to the development control, biosynthesis of several compounds, and pigments, the miR156/SPL module also changes the biosynthesis of bixin in annatto, altering the pattern of related proteins indirectly.

2. MATERIALS AND METHODS

2.1 Plant material

The *B. orellana* cv. Piave Vermelha lines overexpressing miR156 (OE::156) were obtained following a well-established *Agrobacterium tumefaciens* based protocol at Laboratório de Cultura de Tecidos Vegetais II, Bioagro, UFV (Faria et al. 2021). Two lines were selected according to the miR156 expression levels. Eight plants of each OE::156 and four wild type (WT) lines were acclimatized as described in Faria et al. (2019a). Then, the plants were transferred to 5 L polyethylene pots with horticultural substrate Tropstrato HT Hortaliças (Vida Verde Indústria e Comércio de Insumos Orgânicos Ltda, Mogi Mirim, Brasil), under greenhouse conditions. The plants were watered daily and maintained under 11/13 h light and 25/16 °C temperature (day/night). All GMO manipulation was held in the Laboratório de Cultura de Tecidos II – Bioagro and in a GMO-adapted greenhouse, following the CTNBio and CIBio-UFV rules (CQB 024/97 (CTNBio nº 19, process nº 01200.002610/9704)).

2.2 Phenotyping

The acclimatized OE::156 lines kept in a greenhouse were evaluated at 15, 30, 45, 60, 75, and 90 days after planting (DAP). The following variables were assessed: total leaf number, plant height (cm), number of phytomers, diameter of the main axis, third leaf length (from petiole insertion to the apical portion of leaf blade), leaf area, and ramification index (total ramification length and main plant axis length) (Morris et al. 2001). For the leaf area, we measured the area of all Nt leaves, and then sampled the leaf area of OE::156 plants, using the same amount of Nt leaves. For estimation of total OE::156 leaf area, we multiply for by 15, since the OE::156 has 15 times more leaves than Nt plants (sampled OE::156 leaf area x 15). All images were analyzed by ImageJ software Ver. 1.43u, National Institute of Health, US) (Schneider et al. 2012).

2.3 RNA extraction and cDNA synthesis

The miR156 and SPL gene family expressions profile were assessed through qRT-PCR in the CFX96 Touch™ Real-Time PCR Detection System (BioRad, Hercules, CA, United States). We used 40 ng of cDNA, 400 nM of primer, SYBR-green Supermix (BioRad), and deionized water ($_{dd}H_2O$) for a final 10 µL reaction volume. The expression data was gathered from four biological replicates, with at least two technical replicates (reactions) for each. Specific primers for miR156 and developmental linked genes were assayed (Table 1). For amplification, the conditions were the following: 95°C for 10 min and 40 cycles under 94°C for 15 s each, and 60°C for 1 min. For gene expression normalization, we used the genes RPS9 (40S ribosomal protein S9) (Table 1). The gene expression quantification was held by the average comparing method of $2^{-\Delta\Delta Ct}$ (Livak and Schmittgen 2001), where the relevant differences were compared by the t-Student test ($P \leq 0.05$).

Table 1 Target genes and primer sequence that will be applied in *B. orellana* Nt and OE::156 lines. R: Reverse primer; F: Forward primer.

Target gene	Primer sequences	Reference
ALDH3H1 F	5’ – TGGTAGATACTTTCAGAGAGG – 3’	Cárdenas-Conejo et al. 2015
ALDH3H1 R	5’ – GTTGGAGCAATCTTCAGC – 3’	Cárdenas-Conejo et al. 2015
ALDH3I1 F	5' – TGGTAGATACTTTCAGAGAGG – 3'	Cárdenas-Conejo et al. 2015
ALDH3I1 R	5' – GTTGGAGCAATCTTCAGC – 3'	Cárdenas-Conejo et al. 2015
CCD1-1 F	5' – TTCTGGCACTTAACGAGGGT – 3'	Cárdenas-Conejo et al. 2015
CCD1-1 R	5' – CCTTAGGATGAGCAGTGAATG – 3'	Cárdenas-Conejo et al. 2015
CCD4-4 F	5' – TACTGCCAAGATGATCTGG – 3'	Cárdenas-Conejo et al. 2015
CCD4-4 R	5' – GCATTGAGGACATGTAATGG – 3'	Cárdenas-Conejo et al. 2015
DXS2a F	5' – CAGGCATGGCTTTCACTT – 3'	Cárdenas-Conejo et al. 2015
DXS2aR	5' – CGGCAAAGGTAGATGAGTATG – 3'	Cárdenas-Conejo et al. 2015
miR156 F	5' – GCGGCGTTGACAGAAGAGAGT – 3'	Faria et al. 2021
miR156 RT	5' – GTTGGCTCTGGTGCAGGGTCCGAGGTATTCGCACCAGAGCCAACGTGCTC –3'	Faria et al. 2021
miR172 F	5' – CCTGAGAGAATCTTGATGATG – 3'	Designed by us
miR172 RT	5' – GTCGTATCCAGTGCAGGGTCCGAGGTATTCGCACTGGATACGACATGCAG – 3'	Designed by us
PSY1 F	5' – CGATGAGGCAGAGAAAGGAG – 3'	Moreira et al. submitted
PSY1 R	5' –TGGCGATACAACAACAAGGA – 3'	Moreira et al. submitted
RPS9 F	5' – ACTTCTCTCTCACCAGTCCGT – 3'	Faria et al. 2021
RS9 R	5'– GCCTTCTTCATGGAGGCCTT – 3'	Faria et al. 2021
SABATH1 F	5' – ACGGAGGAAGCTATCACCA – 3'	Cárdenas-Conejo et al. 2015
SABATH1 R	5' – GACGTGATATTCAGGGGATC – 3'	Cárdenas-Conejo et al. 2015
SABATH3 F	5' – TTATGGCCGTCTCTGAGGT – 3'	Moreira et al. subimitted
SABATH3 R	5' – ACCTGGCACTCCTGATACG – 3'	Moreira et al. subimitted
SABATH4 F	5' – TCCCGTCTACAAATGGCA – 3'	Cárdenas-Conejo et al. 2015
SABATH4 R	5' – AATTTCGGAGATGACCAGG – 3'	Cárdenas-Conejo et al. 2015
SPL 1 F	5' – ACATCCCTTGCGGCATCACA - 3'	Designed by us
SPL 1 R	5' – TCTGCTGACTGGGTCTCCAT - 3'	Designed by us

SPL 2 F	5' – ACTTCAGTGCAGCAAGGCTC - 3'	Designed by us
SPL 2 R	5' – CACGCAAAACTTTCACTGGGC– 3'	Designed by us
SPL 6 F	5' – TCAGGCTTCAACAGGTGGTGT – 3'	Designed by us
SPL 6 R	5' – ACCTTGGTAAATCCCATCGGCA – 3'	Designed by us
SPL 9 F	5' – CTCGGGGTAACCAACCTGAT – 3'	Designed by us
SPL 9 R	5' – ACCACCAGCATCACTGCCTT – 3'	Designed by us
SPL 13 F	5' – CAGCTGAGGGACGGAACCTA – 3'	Designed by us
SPL 13 R	5' – TGGAGGTGTTGTCTGCTTGC – 3'	Designed by us
SPL 16 F	5'– AATGGTCCAACAGCAACGGAG – 3'	Designed by us
SPL 16 R	5' – TGCAGATGACCCATGATGCC – 3'	Designed by us
Universal Reverse	5' – GTGCAGGGTCCGAGG – 3'	Tang et al. 2012
ZDS F	5' – TCCTCTCCATGGGATTCAAG – 3'	Moreira et al. submitted
ZDS R	5' – GACTGAAGGCAAGAGCCAAA – 3'	Moreira et al. submitted
β-LYC1 F	5' – ATTGTCCAGTGCCTTGGTTC – 3'	Cárdenas-Conejo et al. 2015
β-LYC1 R	5' – CCATGCCAATATCGAGGTTC – 3'	Cárdenas-Conejo et al. 2015
β-LYC2 F	5' – TTCAAGGCCAGCTTGATCGT – 3'	Cárdenas-Conejo et al. 2015
β-LYC2 R	5' – GTGTTTGGGTTCGACGAGGA – 3'	Cárdenas-Conejo et al. 2015
ε-LYC2 F	5' – TTGGAAGTCTTGGAGAAGGAC – 3'	Cárdenas-Conejo et al. 2015
ε-LYC2 R	5' – ACTTATCGGCTAATCTGGACTG – 3'	Cárdenas-Conejo et al. 2015

2.4 Hormonal profile

The following hormone levels were quantified: IAA (Indole-3-acetic acid), zeatin, ethylene by ACC (1-Aminocyclopropane-1-carboxylic acid), ABA (abscisic acid), JA (jasmonic acid), and SA (salicylic acid). For this, we collected eight fully expanded leaves (third from apex to base) from each 3-month-old greenhouse-grown WT and OE::156 plants. Leaf samples (approximately 110 mg) were powdered in liquid nitrogen. A 300 µL aliquot of extracting solution (Methanol:Isopropanol:Acetic acid 20:79:1) was added to 1.5 mL microtubes. After that, the samples were vortexed four times for 20 s each and sonicated for 5 min. Then, the samples were maintained under 4°C, for 30 min. The samples were centrifuged (13,000 ×*g* for 10 min at under 4°C). Immediately, 350 µL from the supernatant were collected to a new microtube. The pellet passed again through the same steps from extraction solution to pellet formation and supernatant separation. For hormonal identification and quantification, an LC-MS/MS (Agilent 1200 Infinity Series) coupled to a Triple Quadrupole mass spectrophotometer QqQ (6430 Agilent Technologies) was used as described in Napoleão et al. (2017).

2.5 Bixin content and bixin channels quantification

Bixin contents were quantified according to Napoleão et al. (2017) and Faria et al. (2019a). Approximately 10 mg of freeze-dried leaves were ground in liquid nitrogen, followed by repeated extraction with 300 µL methanol:isopropanol:acetic acid (20:79:1; v/v/v). Samples were vortexed four times for 20 s, sonicated for 10 min, kept on ice for 30 min, centrifuged at 20,000×*g* for 10 min at 4 °C, and the supernatant was collected. Then, the supernatant was filtered (Econofltr PVDF 13mm and 0.2 µm; Agilent Technologies, Santa Clara, CA, USA) and used for liquid chromatography-mass spectrometry (LC-MS) analysis. Samples of the final supernatant (5 µL) were automatically injected into the LC-QqQ MS instrument (Triple Quadrupole 6430; Agilent Technologies, Waldbronn, Germany) equipped with an Eclipse Plus C18 (2.1×50 mm, 1.8 µm) column and a Zorbax SB-C18 guard column (1.8 µm, Agilent Technologies), at 26 °C. The mobile phase consisted of 0.02% acetic acid in water

(solvent A) and 0.02% acetic acid in acetonitrile (solvent B) at a constant flow rate of 300 µL min^{-1}. A linear gradient was applied as follow: 0–3 min with 2%–60% of B, 3–8 min with 60%–99% of B, 8–11 min with 99% of B, 11–12 min with 99% to 2% of B, and 12–15 min with 2% of B. A mass spectrometer electrospray ionization source was used with the following conditions: gas temperature of 300 °C, the nitrogen flow rate of 10 L min^{-1}, nebulizer pressure of 35 psi, and capillary voltage of 4000 V. Bixin was analyzed via multiple reaction monitoring of ion pairs with mass transitions (395/157) and quantified via calibration curves using pure standards (1 to 200 µg and 0.1 to 500 ng, respectively; Sigma-Aldrich, St. Louis, MO, USA). Data were analyzed using Mass Hunter Workstation software (Agilent Technologies).

For bixin channels counting, we photographed the abaxial part of Nt and OE::156_1, and OE::156_4 leaves using a stereomicroscope Olympus SZX7 (Tokyo, Japan) with a Moticam 580 5.0 MP Nikon (Tokyo, Japan). The images were analyzed using ImageJ version 1.49 (Schneider et al. 2012). We quantified bixin channels in three leaf portions: Basal, Medial, and Apical. Then took three different portions of each image. The bixin channels were divided by mm^2.

2.6 Quantification of pigments

Chlorophylls and carotenoid contents were quantified (µg mL^{-1}) following protocols by Wellburn (1994) and Warren (2008). A volume (600 µL) of MeOH 100% was added to 50 mg of freshly frozen macerated leaf samples. The solution was vortexed for 30 s and incubated at 4 ºC under agitation in the dark for 10 min. Later, the samples were centrifuged at 12000 x *g* (4 ºC, 10 min), and the supernatant was collected. Then, the same procedure was repeated to the remaining pellet, and the supernatant was collected and mixed with the first extraction. After extractions, we collected supernatant (200 µL) and added it to a microplate for absorbance readings (A) at wavelengths of 470, 653, and 666 nm in a Multiskan FC microplate. The contents of total chlorophylls (Chl *a* + Chl *b*) and carotenoids were determined according to the following equations:

$$\text{Chl } a = (15.65 \times \text{A}_{666}) - 7.34 \times \text{A}_{653})$$

$$\text{Chl } b = (27.05 \times \text{A}_{653}) - (11.21 \times \text{A}_{666})$$

$$\text{Carotenoids} = \frac{(1000 \times \text{A}_{470}) - (2.86 \times \text{Chl } a) - (129.2 \times \text{Chl } b)}{221}$$

We also quantified anthocyanins as described by Neff and Chory (1998). The same samples were used as previously mentioned, however using the wavelengths 657 and 530 nm. The relative anthocyanin content was expressed as $(A_{530} - A_{657})\ g^{-1}$ of fresh weight (FW).

2.7 Proteomic extraction and analyzes

For proteomic quantification, leaf samples from each of three different not-transgenic and OE::156_4 plants. We chose just one transgenic line because both independent lines had similar growth, gene expression, pigments, hormone profile, and bixin content. We collected 10 mg of freeze-dry pulverized mass in liquid nitrogen and added 1 mL of extraction buffer, which consisted of 7 M urea (GE Health- care), 2 M thiourea (GE Healthcare, Piscataway, NJ, USA), 2% Triton X-100 (GE Healthcare), 1% dithiothreitol (DTT, GE Healthcare, Piscataway, NJ, USA), 1 mM phenylmethanesulfonyl fluoride (PMSF, Sigma-Aldrich), and complete protease inhibitor cocktail (Roche Diagnostics, Mannheim, Germany). Then, we vortexed and centrifuged the mixture. Then, we collected the supernatants and measured the protein concentration using the 2-D Quant Kit (GE Healthcare, Piscataway, NJ, USA) (Reis et al. 2021). After that, we precipitated the protein samples using the methanol/chloroform methodology to remove any interferents from the samples (Nanjo et al. 2012). Then, we resuspended the samples in a solution consisting of 7 M urea and 2 M thiourea, and protein digestion was performed using Microcon-30 kDa filter units (Millipore) with

the filter- aided sample preparation (FASP) methodology described by Wiśniewski et al. (2009), with some modifications. After digestion, the resulting peptides were quantified with the A205 nm protein and peptide methodology using a NanoDrop 2000c spectrophotometer (Thermo Fisher Scientific) and then injected into a nanoAcquity UPLC mass spectrometer connected to a Q-TOF SYNAPT G2-Si instrument (Waters, Manchester, UK).

The spectra processing and database search were performed using Protein Lynx Global SERVER (PLGS) software v.3.02 (Waters), and label-free quantification analyzes were performed using ISO Quant software v.1.7 (Distler et al. 2014). Only proteins present in at least four runs for differential abundance analysis were considered, aiming to secure high quality results after data processing. A protein abundance differentiation was considered if the fold change value was higher than two, using the Student's t-test (two-tailed, $P \leq 0.05$) and after p-value correction with the Benjamini-Hochberg test. For Functional annotations, we used the Blast2Go software v.5.0 (Conesa et al. 2005) and UniProtKB (www.uniprot.org). A Kyoto Encyclopedia of Genes and Genomes (KEGG) enrichment pathway analysis between DAPs ($P \leq 0.01$) was performed in Metascape (Zhou et al. 2019) after a BLAST search of NCBI (https://www.ncbi.nlm.nih.gov) to obtain *Arabidopsis thaliana* reference sequences.

3. RESULTS AND DISCUSSION

3.1 miR156/SPL module affects architecture and leaf shape in *B. orellana*

B. orellana does not present an apparent phase shift from juvenile to adult, as described by Baliane (1982). To determine whether the master regulator of vegetative phase change miR156/SPL module is functional in *B. orellana*, we characterized OE::156 plants. These plants were grown autotrophically under greenhouse conditions after initial *in vitro* heterotrophic culture. We took care of choosing *in vitro* plants with similar architecture and ramification patterns to avoid any bias that would affect the next growth steps. As depicted in Figure 1A, after 90 days, OE::156 plants showed a strong correlative inhibition, changing drastically stem and canopy growth patterns, with multiple shoots arising from axillary buds. In addition, we observed that OE::156 plants have smaller leaves with different blade shapes as compared to their juvenile non-transformed (Nt) counterparts (Figure 1B). A similar pattern was observed in potato (*Solanum tuberosum*) plants overexpressing miR156, exhibiting more branches from axillary buds, increased number of nodes, smaller leaves with less leaflet number than the non-transgenic counterpart (Bhogale et al. 2014). The same phenomenon was observed in overexpressing miR156 switchgrass (*Panicum virgatum* L.) plants. Otherwise, overexpressing SPL4, a target of miR156, the authors observed fewer auxiliary buds then Nt counterparts (Gou et al. 2017). In poplar (*Populus* sp.), also a woody plant species with subtle phase changes, authors reported more buds and ramification in OE::156 plants, and they were able to see phase change conformations (Rubinelli et al. 2013; Lawrence et al. 2020a). After these first plant architecture observations, we next analyzed plant biometric data in a more detailed way to look into *B. orellana* development and the miR156/SPL module responsiveness.

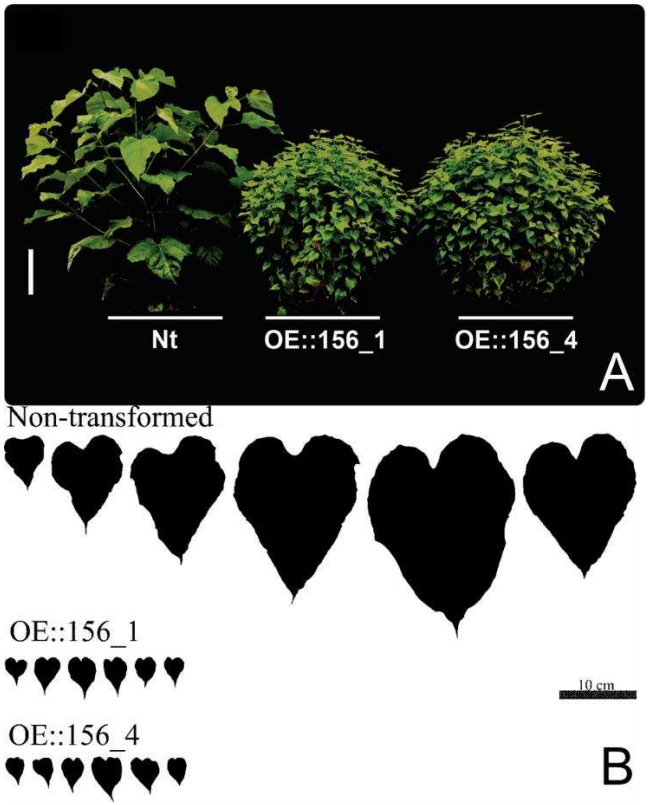

Figure 1. miR156 modulation of growth pattern in *B. orellana*. **A** - Architecture and size of non-transformed plants and plants overexpressing mRNA156 (OE::156) in two distinct lines (OE::156_1 and OE::156_4) at the 90th day after planting in greenhouse. Bar = 10 cm; **B** - Leaf shape and size of non-transformed plants and plants overexpressing mRNA156 in two distinct lines: OE::156_1 and OE::156_4 Bar: 10 cm. Leaves from left to right: First to the sixth leaf, where from three are shown fully expanded leafs.

3.2 miR156/SPL module shapes *B. orellana* biometric features

To understand what features miR156/SPL module was shaping in *B. orellana* plants, we evaluated biometric parameters of plants grown in the greenhouse every 15 days until the 90th day. As expected, both OE::156 lines showed more leaves than their non-transformed counterparts (Figure 2A). We assumed this because miR156 regulates SPL proteins, which upregulate one of many genes related to leaf initiation, *AUXIN-REGULATED GENE INVOLVED IN ORGAN SIZE* (ARGOS), inhibiting leaf initiation in Arabidopsis and Poplar (Hu et al. 2003; Kuluev et al. 2016). Besides, we observed a higher phytomer number in both transgenic lines 30 days onwards under greenhouse (Figure 2B). In addition, we quantified the branching ratio (Figure 2C). Both OE::156 lines had 11-fold more branches than Nt plants. This phenomenon happens as seen in *Petunia axillaris* and *Petunia inflata* plants overexpressing miR156/miR157 (Zhou et al. 2021).

Then, the main stem height of these plants was considered (Figure 2D). We found out that OE::156 plants were higher than Nt plants until the 75th day after planting. The Nt plants were capable to surpass the OE::156 plants on the 90th day and showed statistical difference when compared to OE::156_4. These differences in height could be attributed to less investment in secondary growth showed in OE::156 plants, as seen in main stem diameter (Figure 2E), where in most of the sampled times Nt exhibited significantly higher values than OE::156 plants. A similar pattern was observed in poplar plants, where non-transformed plants were higher than those overexpressing miR156, even though without differences in trunk diameter (Rubinelli et al. 2013).

The first expanded leaf is informative of the physiological status of the plants, in particular of nutrition, hormone regulation, biotic and abiotic stresses status (Lin et al. 2010; Wang et al. 2014). In *B. orellana*, the first observed fully expanded leaf is the third leaf. So, we used to further analysis. We found that on the 15th day, the transgenic lines grew more quickly than Nt plants, but were surpassed on the 45th day (Figure 2F). This can be explained by regulations on organ size under the response of some genes. Such genes are regulated by the miR156/SPL module and very well reported

elsewhere (Zhang et al. 2015; Fouracre and Poethig 2019; Fang et al. 2021). This basal to apical leaf length analysis was important to avoid damaged leaves and altered shoot architecture between transgenic and non-transgenic plants. Therefore, we quantified leaf area photographing all Nt plant leaves after the 90th day, in a manner to mitigate any stress that would impact biochemical or molecular analysis. We were able to quantify all Nt leaves area, but unable to do so in OE::156 plants due the high number of leaves. In this way, the total OE::156 leaf area were obtained, measuring the same non-transgenic leaf number. The Nt leaf area was 16 times higher than OE::156 transgenic lines (Figure 2G). However, when we estimated all transgenic leaf areas there were no significant differences (Figure 2H). This data makes sense because if the transgenic lines would not have the leaf dimensions needed to supply such growth, they probably would not grow and develop. In addition, it would probably lead to starvation or nutrient reallocation failures. The OE::156 lines seems to not changed phases and seems to be incapable to mature all their organs and tissues, since we do not observed presence of mature structures as extrafloral nectaries as seem in Nt plants. Besides, OE::156 lines have more leaves but with the same amount of photosynthetic area than Nt counterparts, which was also observed in *Eucalyptus grandis* (Levy et al. 2014), *Solanum tuberosum* (Bhogale et al. 2014), and *Arabidopsis thaliana* (Xie et al. 2017).

Then, we asked if this responsiveness to mir156/SPL module would be related to any phytohormonal changes, since the loss of apical dominance was observed, as revised in Barbier et al. (2017), we suspected that there is less auxin production or/and more cytokinin on OE::156 plants.

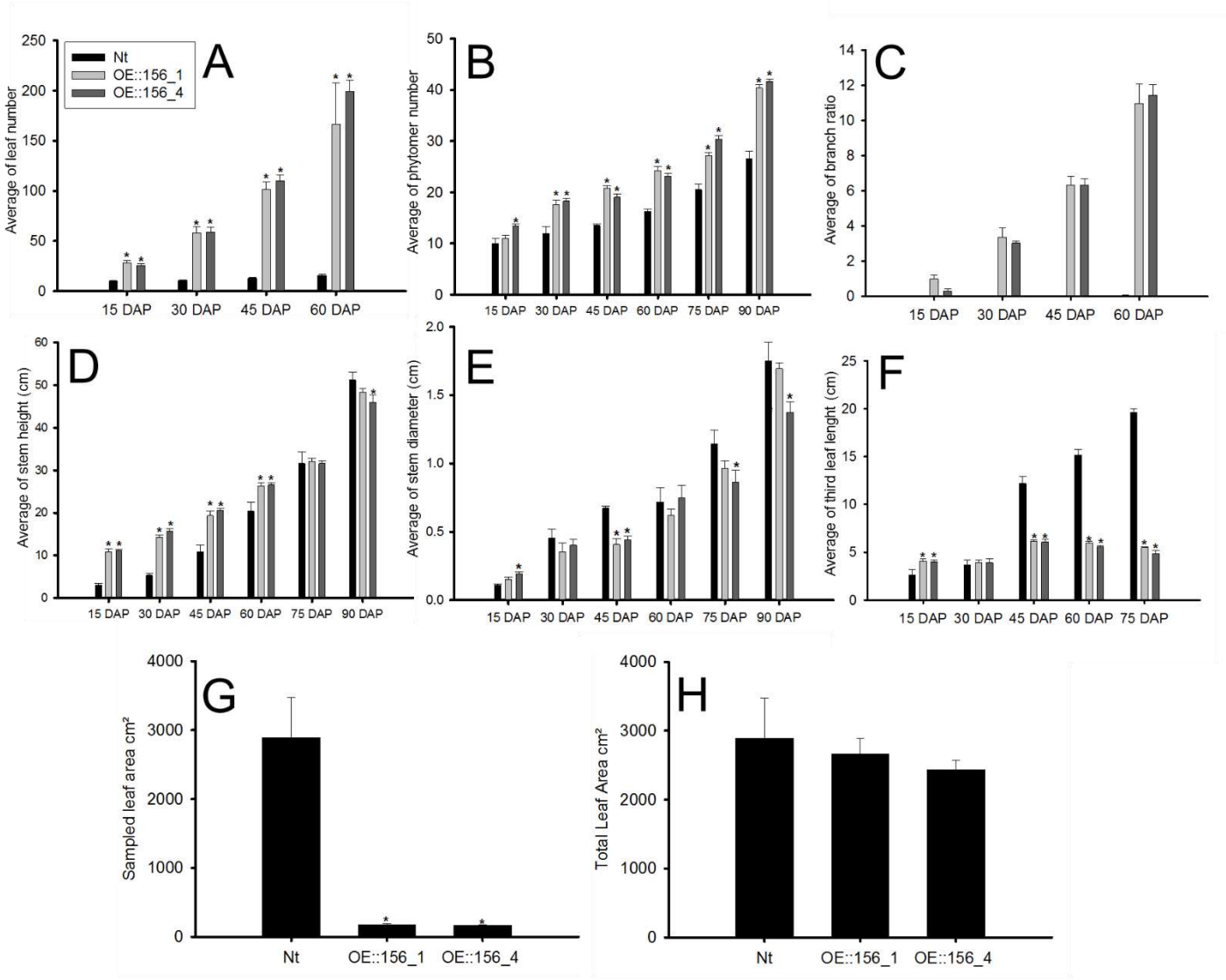
A
Nt
OE::156_1
OE::156_4
Average of leaf number
15 DAP 30 DAP 45 DAP 60 DAP
B
Average of phytomer number
15 DAP 30 DAP 45 DAP 60 DAP 75 DAP 90 DAP
C
Average of branch ratio
15 DAP 30 DAP 45 DAP 60 DAP
D
Average of stem height (cm)
15 DAP 30 DAP 45 DAP 60 DAP 75 DAP 90 DAP
E
Average of stem diameter (cm)
15 DAP 30 DAP 45 DAP 60 DAP 75 DAP 90 DAP
F
Average of third leaf lenght (cm)
15 DAP 30 DAP 45 DAP 60 DAP 75 DAP
G
Sampled leaf area cm²
Nt OE::156_1 OE::156_4
H
Total Leaf Area cm²
Nt OE::156_1 OE::156_4

Figure 2. miR156 impact on biometric features of *B. orellana* plants. **A** - Total leaf number until 60 days after planting (DAP); **B** - Average phytomer number assessed up to 90 DAP; **C** - Branching ratio assessed up to 60 DAP; **D** - Average values for main stem height assessed up to 90 DAP; **E** - Average values for main stem diameter until 90 DAP; **F** - Third leaf length (from petiole insertion to the end of leaf blade) 75 DAP; **G** - Sampled Leaf Area in the 90th DAP (n=20); **H** - Total leaf area [sampled leaf area multiply by number of Nt leaves (15)] in the 90th DAP. DAP: Days after planting in the greenhouse. Asterisks stand for *P*-value ≤ 0.05 using t-Student test; Nt = Non-transformed, OE::156_1 = Plants overexpressing miR156 line 1. OE::156_4 = Plants overexpressing miR156 line 4. Vertical bars correspond to standard error variation.

3.3 miR156/SPL module altered phytohormones endogenous levels

The endogenous phytohormone profiles from Nt and OE::156 plants were characterized by LC-MS/MS. The main hormones were quantified and the results are shown below. The Brassinolides are steroidal plant hormones first isolated from *Brassica napus* pollen grains (Grove et al. 1979). Those hormones are linked to cell elongation and plant growth (Yokota 1997). However, several studies showed the role of brassionolides in plant architecture, abiotic, and biotic stresses, as revised in Coll et al. (2015) and Anwar et al. (2018). Unchanged brassinolide 1 and 2 levels in OE::156 plants (Figures 3A and 3B) are consistent with the stem height data, as OE::156 plants grew alike the Nt in the main stem height feature (Figure 2D), which could be related to brassinolides levels. Other interestingly feature is the relationship between brassinolides and SPL proteins in vegetative phase changes. Brassinolides and SPL proteins act together, whereas plants overexpressing SPL9 were hypersensitive to brassinolides (Wang et al. 2021). However, in SPL downregulated plants (OE::156) the brassinolides seem to display the same pattern as Nt plants in main stem height but did not contribute to leaf maturation and elongation as seen in leaf length data (Figure 2F). Any interaction between SPL activity and brassinolides may therefore reflect altered sensitivity to brassinolides, rather than upregulation of Brassinolide synthesis.

The ethylene (ET) precursor 1-aminocyclopropane-1-carboxylic acid (ACC) is an effective marker for quantifying ET levels (Avni et al. 1994). In light of this, we measured ACC levels in OE::156 and Nt plants. We observed that ACC was slighter higher in OE::156_4 plants than its Nt counterparts but this level was not statically significant (Figure 3C). ET is also indirectly responsible for vegetative phase changes, regulating SPL through DELLA (aspartic acid–glutamic acid–leucine–leucine–alanine) proteins, activating miR172 and consequently APL2 proteins (Vanstraelen and Benková 2012; Wang 2014; Wang and Wang 2015). In contrast, the contrary is not true; the overexpression of miR156 seems not to have changed the ET production in *B. orellana*.

Methyl jasmonate (MeJA) and jasmonic acid (JA) are very important for plant development processes, as such: root growth, flowering, fruit ripening, and

senescence, as well-reviewed in Cheong and Choi (2003) and Singh and Dwivedi (2018). Jasmonate is also related to juvenile phase prolongation, since young maize plants displayed higher levels of JA in their leaves, besides that the application of exogenous JA extended juvenile stage duration (Osadchuk et al. 2019). Besides that, with salicylic acid (SA), these phytohormones are responsible for plant defense against pathogens, temperature, salt, among others stress that can activate the immune system of plants (Wani et al. 2017; Yu et al. 2019). Here we quantified both hormones to have clues about any stresses that the plants were suffering. Both MeJA and SA (Figure 3D and 3E) did not differ significantly from control plants. We tried to quantify free jasmonate but the peak areas were too small demonstrating that the JA levels were too low, despite the sensitivity of the LC-MS/MS technique.

In a manner to explain the loss of apical dominance in OE::156 plants (Figure 1A), we quantified cytokinins (zeatins) and auxin (IAA). Cytokinins are related to axillary meristem activation through the adenosine phosphate-isopentenyltransferase (IPT) gene, which will induce cytokinin production in a positive feedback provoking cell differentiation in axillary buds (Shimizu-Sato et al. 2009; Su et al. 2011). Thereby, we quantified the zeatin isoforms 1 and 2 and their isomers, *cis*-Zeatin and trans-Zeatin, referring to the position of the terminal hydroxyl group on the isoprenoid side chain. We observed the same levels of *cis*-Zea 1 (Figure 4A) and *trans*-Zea 2 (Figure 4B) in Nt and OE::156 plants. On other hand, we found significantly higher levels of Zea 2 Cis in OE::156_1 plants than Nt (Figure 4C). Interestingly, OE::156_1 plants showed lower levels of Zea 1 Trans than Nt counterparts (Figure 4D). It goes in the opposite direction because OE::156_1 plants have this divergent plant canopy, with activated axillary buds. The *cis* and *trans*-Zeatin isomers occur in different points of *Arabidopsis thaliana* development (Gajdošová et al. 2011), and several authors attributed different functions for both, from environmental stresses to nitrate metabolism (Schäfer et al. 2015; Lacuesta et al. 2018). In this way, further investigation in Zeatin isomers levels can reveal new functions to c*is*-Zeatin in *B. orellana* plants, suing roots for example, given that SPL10 has interactions with cytokinins in Arabidopsis roots through *ARABIDOPSIS RESPONSE REGULATOR1* (*ARR1*) gene (Barrera-Rojas et al. 2020).

As plant structure depends also on auxin levels, we quantified IAA since it is the main form of this phytohormone in plants (Mashiguchi et al. 2011). Interestingly, we found higher levels of auxin in both OE::156 plants than the Nt (Figure 5A). Such data

do not match with our first hypothesis of loss apical dominance by low levels of auxin in the whole plant, a well-studied process as reviewed by Barbier et al. (2017). These findings contradict previous studies that found a negative correlation between miR156 expression and auxin levels, as seen in rice, where overexpressing miR156 plants showed more tillers and therefore lowest auxin levels (Dai et al. 2018). May auxin levels are higher because of the interplay auxin-cytokinin. Since OE::156 plants seems to have higher levels of cytokinin in the leaf cells, the auxin production is also higher, but with the *PIN-FORMED* (PIN) proteins in lower expression levels. Therefore, the auxin is not being transported from leaf cells. The SPL10 is a miR156 target and controls the cell cycle as shown in rice (Barrera-Rojas et al. 2020). This protein is also responsible for cytokinin levels (Yu et al. 2015a). Consequently, the lack of SPL10 activity seems to activate cytokinin production and indirectly decrease PIN protein expression lowering auxin transports from this region. Such auxin-cytokinin interplay is reviewed well reviewed elsewhere (Su et al. 2011).

To further explore the interesting development pattern of OE::156 plants, we quantified gibberellic acid (GA) content in Nt and OE::156 plants Figure 5B and 5C. We chose GA_3 and GA_4 because of their higher bioactivity among other gibberellins (Gupta and Chakrabarty 2013). Interestingly, we observed lesser levels of GA_3 and GA_4 in OE::156_4 plants than in non-transformed line. In garlic, GA_3 applied exogenously was responsible for more secondary stems in the plant architecture that takes after OE::156 *B. orellana* plants (Liu et al. 2019). However, in Petunia (*Petunia* sp), GA insensible transgenic lines showed more branches, shorter leaves, and shorter plants than non-transformed lines (Liang et al. 2014). In addition, in Arabidopsis, the SPL proteins interact with DELLA proteins, degrading it and amplifying GA signaling (Jung et al. 2012; Yu et al. 2012). Therefore, SPL defective plants may have downregulated GA biosynthesis genes due to the lack of DELLA proteins (Ito et al. 2018), which could explain why OE::156 plants had higher heights in the first 60^{th} days and then were surpassed by Nt plants in the 90^{th} day (Figure 3D).

Abscisic Acid (ABA) is a plant hormone responsible for a series of developmental processes, such as cell division and elongation, and floral induction (Finkelstein 2013). Thus, we quantified ABA levels in OE::156 and Nt leaves (Figure 5D). We observed 2-fold higher ABA levels in OE::156_1 plants and 1.6-fold higher in OE::156_4 plants than Nt plants. This result was brought to our attention since ABA

could compete with bixin production. The Bixin is an apocarotenoid that is converted from Lycopene through *Carotenoid cleavage dioxygenase 4* (CCD4) activation (Cárdenas-Conejo et al. 2015). However, the Lycopene is also a precursor of β-carotene by *Lycopene cyclase 2 beta* (β-LYC), transposing the carbons to the xanthins route, which results in Neoxanthin production. The Neoxanthin is oxidatively cleaved by the *9-cis-epoxycarotenoid dioxygenase* (NCED) enzyme, producing xanthoxin and then ABA (Chen et al. 2020). To distinguish between the different lycopene metabolic pathways, we investigated the effects of constitutive miR156 expression on bixin production.

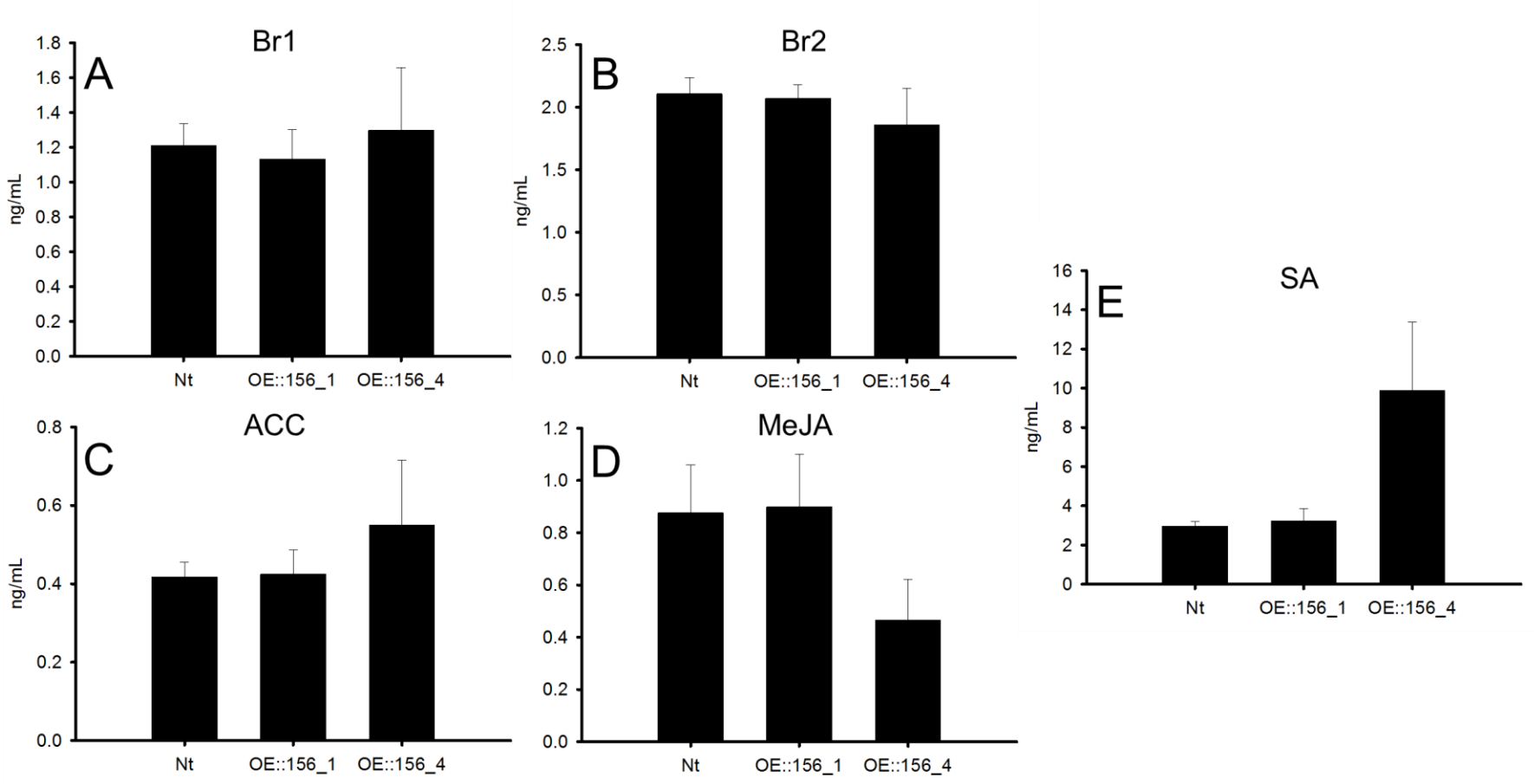

Figure 3. Average values for endogenous hormone levels in transformed and non-transformed *Bixa orellana* plants at the 90th day of growth under greenhouse conditions. **A** - Brassinolide 1 (Br1) ; **B** - Brassinolide 2 (Br2); **C** - 1-aminocyclopropane-1-carboxylic acid (ACC); **D** - Methyl jasmonate (MeJA) average levels; **E** - Salicylic Acid (SA). The results are adjusted to fresh leaf masses from four

plants of each line, where Nt = Non-transformed, OE::156_1 = Plants overexpressing miR156 line 1. OE::156_4 = Plants overexpressing miR156 line 4. Vertical bars correspond to standard error variation.

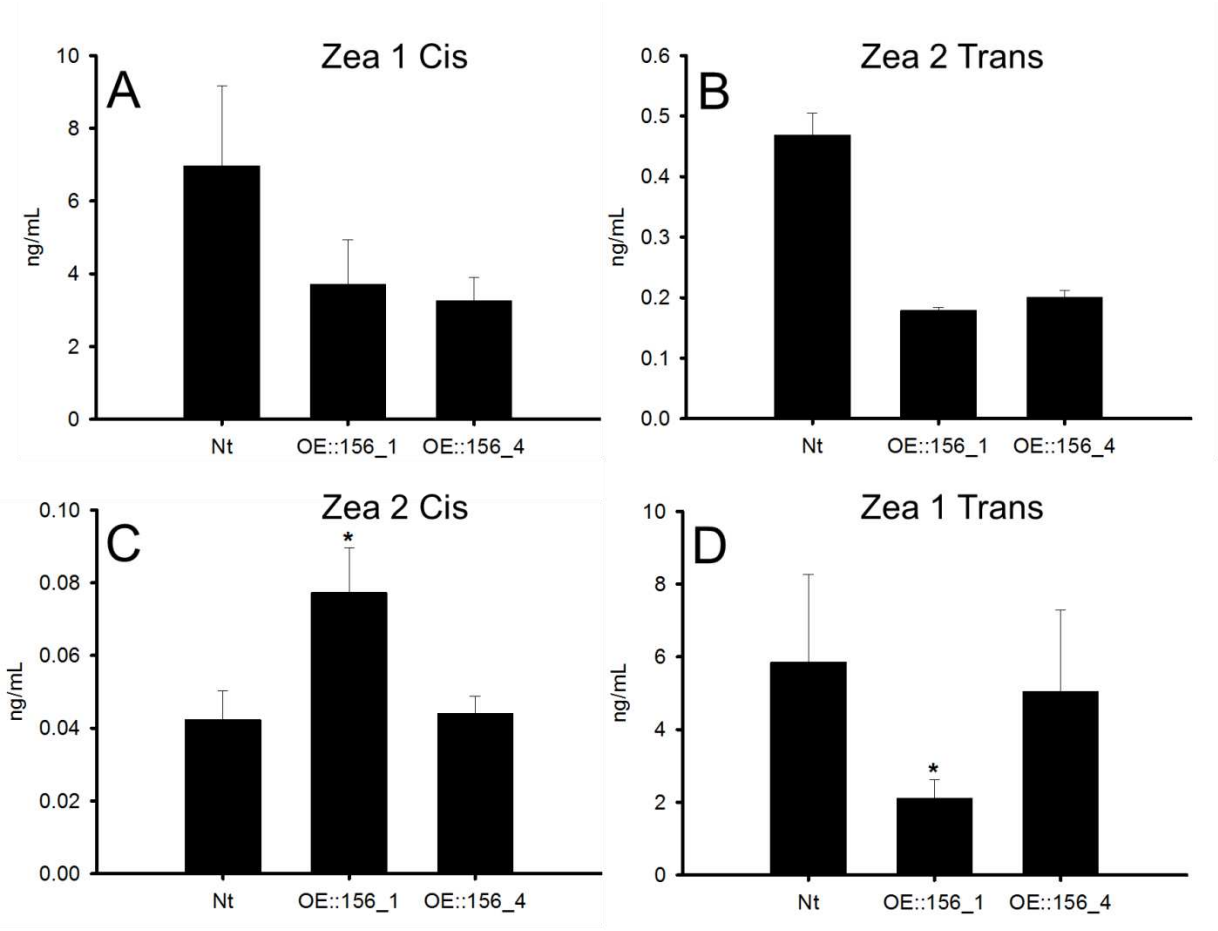

Figure 4. Average values for endogenous cytokinins levels in transformed and non-transformed *Bixa orellana* plants at the 90th day of growth under greenhouse conditions. **A** - *Cis*-Zeatin 1 (Zea 1 Cis); **B** - *Trans*-Zeatin 2 (Zea 2 Trans) average levels; **C** - *Cis*-Zeatin

2 (Zea 2 Cis); **D** - *Trans*-Zeatin 1 (Zea 1 Trans). Asterisks stand for *P*-value ≤ 0.05 using student-t test. Nt = Non-transformed, OE::156_1 = Plants overexpressing miR156 lin 1. OE::156_4 = Plants overexpressing miR156 line 4. Vertical bars correspond to standard error variation.

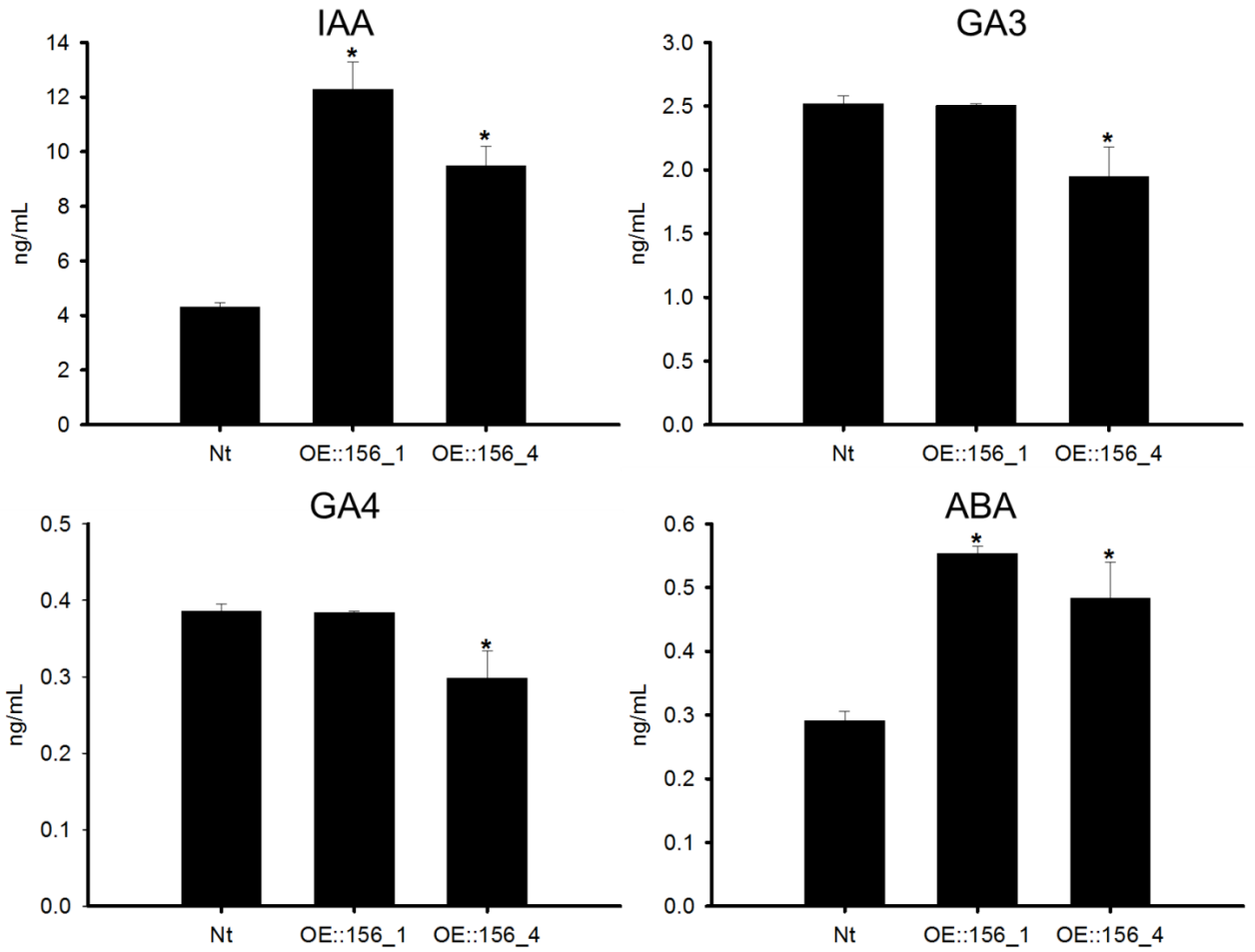

Figure 5. Average values for endogenous hormone levels in transformed and non-transformed *Bixa orellana* plants at the 90th day of growth under greenhouse conditions. **A** - Indole-3-Acetic Acid (IAA); **B** - Gibberellic Acid 3 (GA_3); **C** - Gibberellic Acid 4 (GA_4); **D** - Abscisic Acid (ABA). Asterisks stand for *P*-value ≤ 0.05 using student-t test. Nt = Non-transformed, OE::156_1 = Plants overexpressing miR156 line OE::156_4 = Plants overexpressing miR156 line 4. Vertical bars correspond to standard error variation.

3.4 Transgenic plants overexpressing miR156 have reduced bixin content

The higher ABA levels and the possible carotenoid bixin relationship is intringing, so the main pigments were quantified in OE::156 and Nt plants (Table 2). We observed that the amount of carotenoids, chlorophylls (*a* and *b*), and anthocyanins did not differ among them. This result does not match with previous data in Arabidopsis, where anthocyanins accumulated in miR156 overexpressing plants, since SPL9 prevents the expression of anthocyanin biosynthesis-related genes (Gou et al. 2011). Additionally, overexpressing miR156 Poplar plants, also displayed higher levels of anthocyanins, flavonols, and flavonoids than their Nt counterparts (Wang et al. 2020b). These results in *B. orellana* overexpressing miR156 could be a response to the greenhouse environment, where plants are growing in a natural light condition, differently from the two studies cited that used artificial light (Gou et al. 2011; Wang et al. 2020b). In addition, the miR156/SPL module is not the only mechanism of anthocyanin biosynthesis responses. This pigment biosynthesis can be up or down-regulated by temperature, sugars, hormonal signaling, among other factors (Das et al. 2012; LaFountain and Yuan 2021).

Nevertheless, our main objective was to understand how this miR156 overexpressing *B. orellana* plants are delivering their carbon to ABA biosynthesis instead of synthetize bixin. As expected, the miR156 overexpressing plants displayed 2.5-fold less bixin than both transformed plants (Figure 6A). Our first thought was then to quantify the bixin channels in the abaxial face of the leaves (Figure 6B and 6C). We observed that in the basal part of the leaf, OE::156 and Nt leaves had the same amount of bixin channels. However, in the medial and apical parts, Nt leaves showed more bixin channels, since such structures needs structural maturation and the miR156/SPL module is directly involved in leaf development through *Wuschel/Clavata* genes, as shown in Arabidopsis (Fouracre and Poethig 2019). Therefore, it is likely that SPL proteins promote the formation of bixin channels. As demonstrated, the bixin channels are develop as laticifer pigment glands which cells gradually coalesce with adjacent cells and only shared cell walls are degraded (Almeida et al. 2021)

Table 2. Total content of clorophyll *a* (Chl *a*) and *b* (Chl *b*), carotenoids, and anthocyanin adjusted by fresh weight in Nt (non-transformed) and OE::156 (OE::156_1 and OE::156_4) leaves of *Bixa orellana* plants.

Line	Chl *a* (µg mg^{-1})	Chl *b* (µg mg^{-1})	Carotenoids (µg mg^{-1})	Chl *a*/*b* (µg mg^{-1})	Anthocyanin (A_{530} - A_{657}) g^{-1})
Nt	0.034 ± 0.0005	0.034 ± 0.0006	0.235 ± 0.0187	1.006 ± 0.0257	0.002 ± 0.0001
OE::156_1	0.062 ± 0.0137	0.055 ± 0.0102	0.227 ± 0.0296	1.104 ± 0.0876	0.002 ± 0.0003
OE::156_4	0.030 ± 0.0018	0.032 ± 0.0012	0.216 ± 0.0086	0.923 ± 0.0306	0.002 ± 0.0005

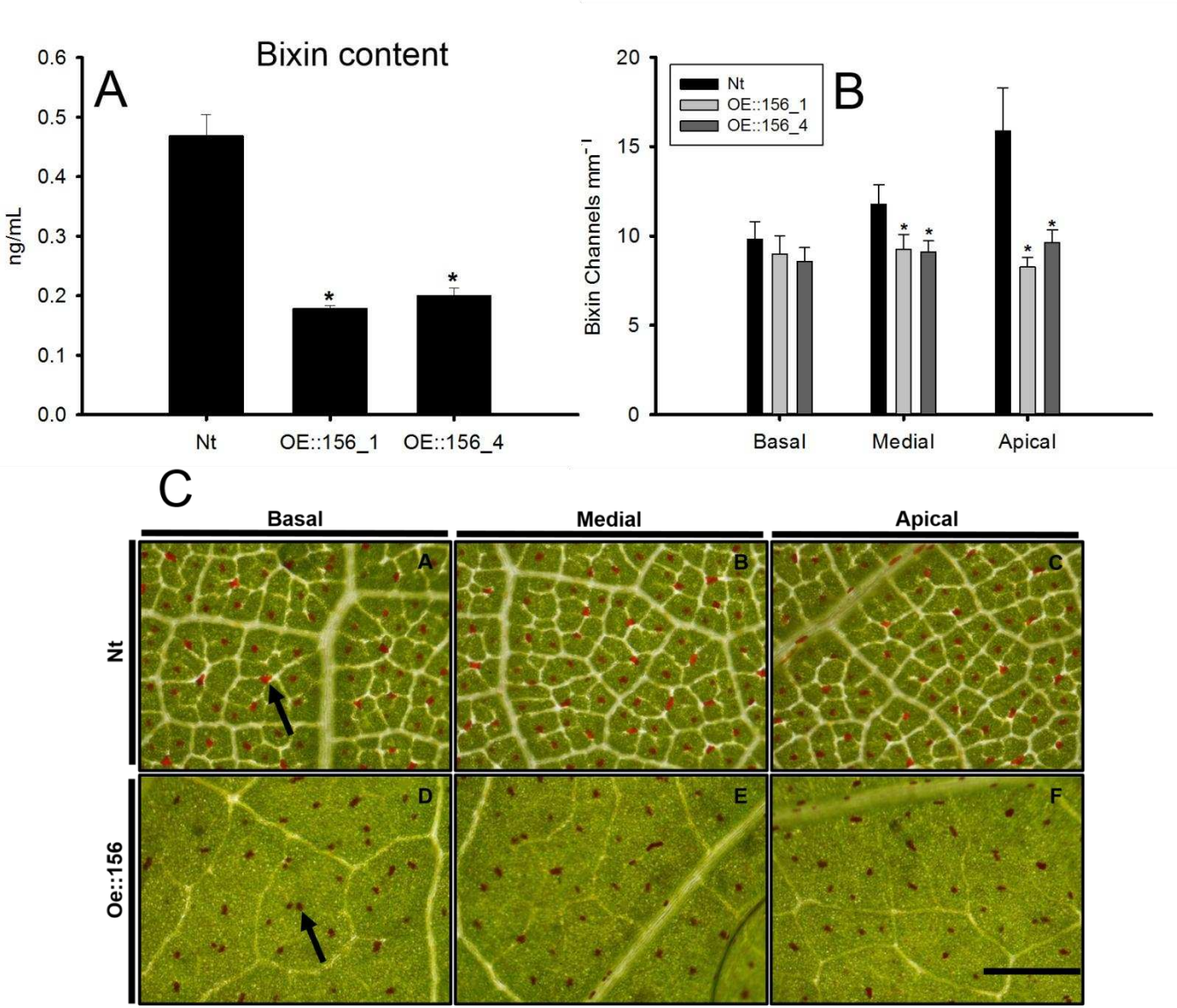
A
Bixin content
ng/mL
0.6
0.5
0.4
0.3
0.2
0.1
0.0
Nt
OE::156_1
OE::156_4
B
Nt
OE::156_1
OE::156_4
Bixin Channels mm⁻¹
20
15
10
5
0
Basal
Medial
Apical
C
Basal
Medial
Apical
Nt
Oe::156
A
B
C
D
E
F

Figure 6. miR156 modulation of bixin related features in *B. orellana*. **A** - Total bixin content average values in *B. orellana* plants at 90th DAP. The results are adjusted to fresh leaves mass of four plants of each line; **B** - Average number of bixin channels in different *B. orellana* abaxial leaf parts (Basal, Medial and Apical) at 180th DAP; **C** - Detailed bixin channels (Basal, Medial and Apical) in *B. orellana* leaves at 180th DAP. The arrows indicate the bixin channels in the abaxial face of the leaf blade. DAP = Days after planting in the greenhouse Nt = Non-transformed, OE::156_1 = Plants overexpressing miR156 line 1. OE::156_4 = Plants overexpressing miR156 line 4. Asterisks stands for *P*-value ≤ 0.05 using student-t test. Bar = 1 cm. Vertical bars correspond to standard error variation.

3.5 OE::156 plants have different bixin related gene expression pattern

At the vegetative stage, plants have to pass from juvenile to adult. This process is mediated by miR156, which controls SPL, a family of transcription factors responsible for starting the phase change phenomenon (Wu and Poethig 2006; Wu et al. 2009). Our *B. orellana* OE::156 plants were obtained through *A. tumefaciens* transformation and characterized as miR156 overexpressing plants and, consequently, with SPL defective expression, using qRT-PCR analyzes (Faria et al. 2021). However, to be sure that this profile would continue in the greenhouse, we analyzed the miR156 and miR172 levels (Figure 7A and 7B). As expected the miR156 levels were higher in both OE::156 lines than its Nt counterparts, and the contrary was true to miR172.

The levels of miR172 were lower in OE::156 plants, which is important because this result is compatible with fewer bixin channels in OE::156 plants since miR172 is responsible for leaf cell maturation as seen in Rice (Zhu et al. 2009), Arabidopsis (Jung et al. 2011), and *Passiflora* (Silva et al. 2019). It is compatible with previous studies where miR156 represses miR172 activity through SPL destabilization, as reviewed by Liu et al. (2018).

Then, we proceed with SPL expression levels quantification. All SPLs assessed were identified from a transcriptome (Moreira et al., submitted), and were further confirmed as orthologs from Arabidopsis SPLs (data not shown). As foreseen, SPL1 has been suppressed in both OE::156 plants (Figure 8A). In switchgrass, SPL1 is involved in tiller initiation rather than phase change (Wu et al. 2016). Compared to our OE::156 plants, it could start to explain why we observed a higher branching ratio (Figure 2C).

We also quantified SPL6 mRNA abundance and we observed lower expression levels in both OE::156 plants (Figure 8B). The SPL6 function is linked to cell death, for example, in rice, authors have observed cell death in the panicle apical region (Wang et al. 2018). Our plants may have the same patterns in a few branches, which could contribute to lateral canopy growth in OE::156 plants.

In addition, we quantified SPL9 mRNA levels. The SPL9 levels were significantly lower in OE::156_1 but not in OE::156_4 (Figure 8C), which could be explained by the RT-qPCR quantification method. The miR156 could destabilize SPL9

mRNA in portions where the RT-qPCR primer still could anneal with its target and generate a false greater transcripts abundance since this is a major problem for miRNA identification (Hausser and Zavolan 2014).

Another important SPL protein is the SPL13, which is related to stress regulation. In alfalfa (*Medicago sativa* L.), overexpression of miR156 and silencing of SPL13 was capable to enhance drought tolerance through stomata sensitivity (Arshad et al. 2017). Also in alfalfa, SPL13 was capable to regulate *Dihydroflavonol-4-reductase* (DFR), which is linked to anthocyanin production, binding to its promoter (Feyissa et al. 2019). In addition, SPL13 seems to be involved in drought tolerance specific tissue targets, as shown by Feyissa et al. (2020). SPL13 defective plants displayed different genes expression patterns related to water deficit, such as acyl-CoA dehydrogenase, ubiquinol-cytochrome-c reductase, and hydroxymethylglutaryl-CoA reductase (NADPH) activity, mainly in the stems than in leaves or roots. It demonstrates how SPL13 could be involved in modulating secondary metabolism in alfalfa. In the light of this, we quantified SPL13 (Figure 8D), in a manner to see how this gene could be involved in the bixin reduction. A 2.5-fold fewer transcripts were detected in OE::156 plants. Such results shed light on how OE::156 *B. orellana* plants could be more tolerant to drought, activating physiological and metabolic processes, leading to further studies with these plants.

In rice, SPL16 is related to grain filling and size by cell cycle regulation. Overexpression of SPL16 in these plants resulted in a proliferation of endosperm cells and grain yield by 13.5% (Wang et al. 2012). Besides that, SPL16 is also related to abiotic stress responses. In poplar roots exposed to salt stress, SPL16 expression was 2-fold upregulated (Guo et al. 2021). Moreover, in banana (*Musa acuminata*), SPL16 was responsible for secondary metabolism regulation. The authors observed that this transcriptional factor regulates lycopene β-cyclase (β-LYC) in fruits, where SPL16 enhanced transcription leads to upregulation of β-LYC and, consequently, more β-carotene in such fruits (Zhu et al. 2020). Thereby, we quantified SPL16 expression in OE::156 and Nt *B. orellana* (Figure 8E). 7-fold fewer transcripts were found in transgenic lines. These results are a piece of evidence of how the bixin production is affected by the miR156/SPL module since it is related to carotenoid production.

Our research group joined a transcriptomic profile analysis of different *B. orellana* seed stages (Moreira et al. submitted). The transcriptome-derived information

was a relevant foundation to better understand how the miR156/SPL module was interfering in bixin biosynthesis. The bixin is an apocarotenoid and its precursor is the same as the carotenoid pathway, the glyceraldehyde-3-phosphate (GADP) and pyruvate. The first step is the conversion GADP to 1-deoxy-d-xylose-5-phosphate (DXP) by 1-deoxy-D-xylose-5-phosphate synthase 2a (DXS2a) (Vaccaro et al. 2014). In this way, the levels of DXS2a transcripts were quantified (Figure 9A). A 4-fold fewer transcripts in OE::156_1 was detected as compared to Nt plants. However, the OE::156_4 line did not differ from the control. Such difference between the two transgenic lines is a piece of evidence that the bixin production is regulated downstream of its pathway.

The next analyzed step was the conversion of dimethylallyl pyrophosphate (DMAPP) into phytoene by phytoene synthase 1 (PSY1) (Fu et al. 2014). We quantified the mRNA of this enzyme, since it is present in various tissues and organs, and is responsive to abiotic stresses as well (Kaur et al. 2017). Our transgenic lines had 2.8-fold fewer transcripts, on average, than Nt plants (Figure 9B). It is an important result because showed that the carotenoid biosynthesis route is being suppressed. However, we still asked how and at which point ABA biosynthetic pathway was upregulated. To address it, we quantified the Zeta-carotene desaturase (ZDS) mRNA levels (Figure 9C). Interestingly, OE::156 ZDS transcription does not differ from Nt plants. ZDS is a key enzyme not only in the lycopene biosynthesis but in chloroplast development as well. In maize, ZDS defective mutants showed albino and lethal phenotypes, demonstrating that ZDS also upregulates other chloroplast genes linked to photosynthesis affecting grana, stroma, and thylakoids arrangement, showing markedly reduced and irregular membranes (Wang et al. 2020a). As we did not see such behavior in OE::156 plants, the mir156/SPL module seems not to affect ZDS expression.

Since lycopene is also a precursor of ABA biosynthesis, we quantify the Carotenoid cleavage dioxygenase 4 (CCD4-4) mRNA levels (Figure 9D). We observed 2-fold less expression in OE::156_1 and 6-fold less transcription in OE::156_4 than Nt line. According to the Moreira *et al*. model (submitted), CCD4-4 is the enzyme responsible for lycopene cleavage in bixin aldehyde, which would proceed in the bixin route. In chrysanthemum (*Chrysanthemum morifolium* Ramat.), defective CCD4-4 led to white petals. These plants showed carotenoid production by other enzymes from the

same family but these carotenoids were further degraded and did not take part in coloring the petals (Ohmiya et al. 2006). Then, we further analyzed the bixin route to see if this was the breaking point for this carotenoid biosynthesis.

The SABBATH methyltransferases family seems to methylate norbixin to produce bixin. In this way SABBATH proteins are the ending point of bixin production (Cárdenas-Conejo et al. 2015; Faria et al. 2020). Here we quantify SABBATH 1, 3, and 4 (Figures 10A, 10B, and 10C). We noticed that all tested SABBATHs were downregulated in OE::156 plants. However, the SABBATH 1 was mostly repressed, almost 8-fold in both transgenic lines. It can be due to the lack of bixin aldehyde and further norbixin, substrates for bixin production.

Aldehyde dehydrogenase family 3 member I1 (ALDH3I1) is responsible to transform bixin aldehyde to norbixin. Here, we quantified its transcripts through RT-qPCR. We found that OE::156_1 plants presented lesser ALDH3I1 gene expression than Nt plants (Figure 10D). Nonetheless, OE::156_4 plants did not show the difference from the control plants. Therefore, we tested another ALDH enzyme, the Aldehyde dehydrogenase family 3 member H1 (ALDH3H1) (Figure 10E). We found that both transgenic lines showed lower gene expression than Nt plants. The ALDH3 family is regulated by the ABA stress response pathway, so we could have seen a response for higher ABA levels (Figure 5D) in these two gene transcripts rather than see a direct or indirect involvement of the miR156/SPL module (Brocker et al. 2013). Despite this, the ALDH superfamily has other functional characteristics in plants, as shown in arabidopsis, where ALDHs played a central role, through putrescines and 4-aminobutyrate (GABA) production, in salt tolerance (Zarei et al. 2016), which could be less probable it's regulation by miR156/SPL module.

To avoid a dead-end in investigating where the carbons may be going from bixin production to ABA biosynthesis, we tested which enzymes that could be involved in the carbon translocation to this pathway. We quantified the carotenoid cleavage dioxygenase 1 (CCD1) (Figure 11A). This enzyme is responsible to deviates the route from bixin production in *B. orellana* (Cárdenas-Conejo et al. 2015). The results showed that OE::156 plants had 2-fold (OE::156_1) and 2.5-fold (OE::156_4) higher transcription levels than the Nt counterparts. This result is a shred of evidence to which route the carbon, which once would go to bixin production, is going since the bixin is a huge carbon sink (Cazzonelli and Pogson 2010).

After lycopene, the biosynthesis of carotenoid goes through two different pathways, depending on the activity of two enzymes: lycopene *ε*-cyclase (εLCY), which produces alpha-carotenoids; and lycopene β-cyclase (βLCY) to produce beta-carotenoids. As well-reviewed by Cazzonelli and Pogson (2010), this branch point has a major regulatory role in modulating the ratio of the most abundant carotenoid. Bearing in mind, we quantified Lycopene *e*-cyclase 2 (*e*-Lyc2) mRNA levels (Figure 11B). OE::156 plants did not differ from Nt plants, although OE::156 plants showed slightly fewer transcripts. Moreover, we quantified Lycopene β-cyclase 1 and 2 (β –Lyc1 and β -Lyc2) (Figures 11C and 11D). In OE::156_1 plants, β –Lyc1 showed 1.5-fold higher than Nt counterparts. Nevertheless, in OE::156_4 plants the β –Lyc2 was higher than Nt plants. These results show that the main carbon sink may be the xanthin biosynthesis route, where the ABA is synthesized, as far as the hormone profile indicated. Even though, we still asked if the bixin pathway is affected by the miR156/SPL module.

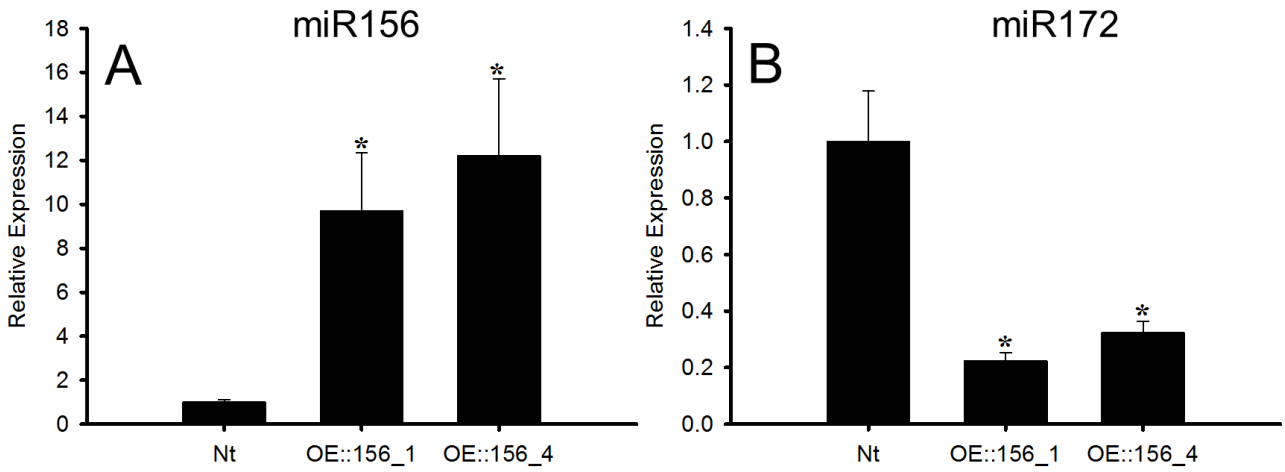

Figure 7. MiRNA transcript levels in *B. orellana* plants at 90th day after planting in the greenhouse. **A** – miR156; **B** – miR172 (B). Nt = Non- transformed, OE::156_1 = Plants overexpressing miR156 line 1. OE::156_4 = Plants overexpressing miR156 line 4. Asterisks stand for *P*-value ≤ 0.05 using student-t test. Vertical bars corresponds to standard error variation.

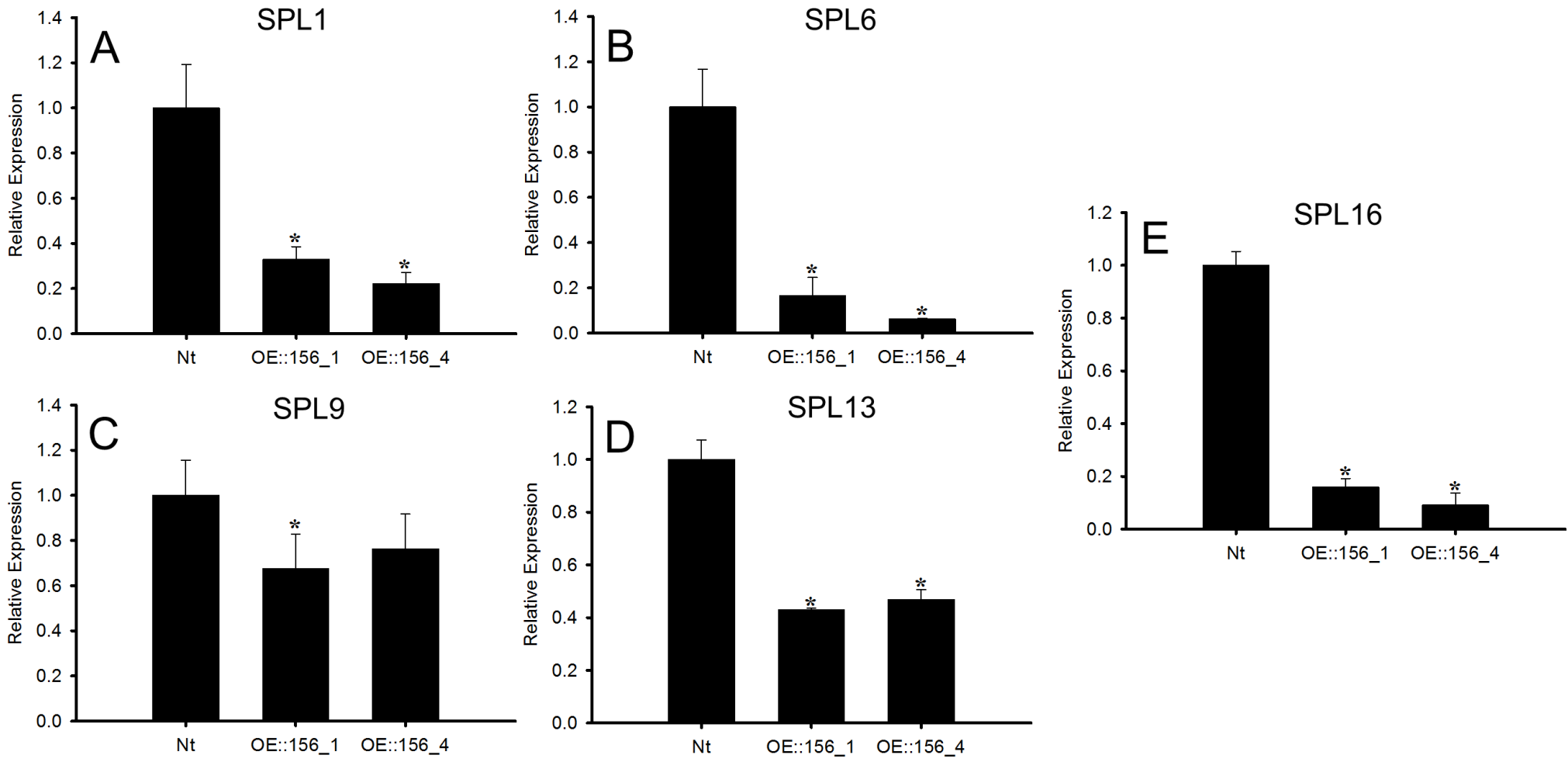

Figure 8. Relative expression levels of *Squamosa promoter binding protein Like* (SPL) genes in *Bixa orellana* plants growing in greenhouse at 90th day. **A** - SPL1; **B** - SPL6; **C** - SPL9; **D** - SPL13; **E** - SPL16. Nt = Non- transformed, OE::156_1 = Plants

overexpressing miR156 line 1. OE::156_4 = Plants overexpressing miR156 line 4. Asterisks stand for *P*-value ≤ 0.05 using t-Student test. Vertical bars correspond to standard error variation.

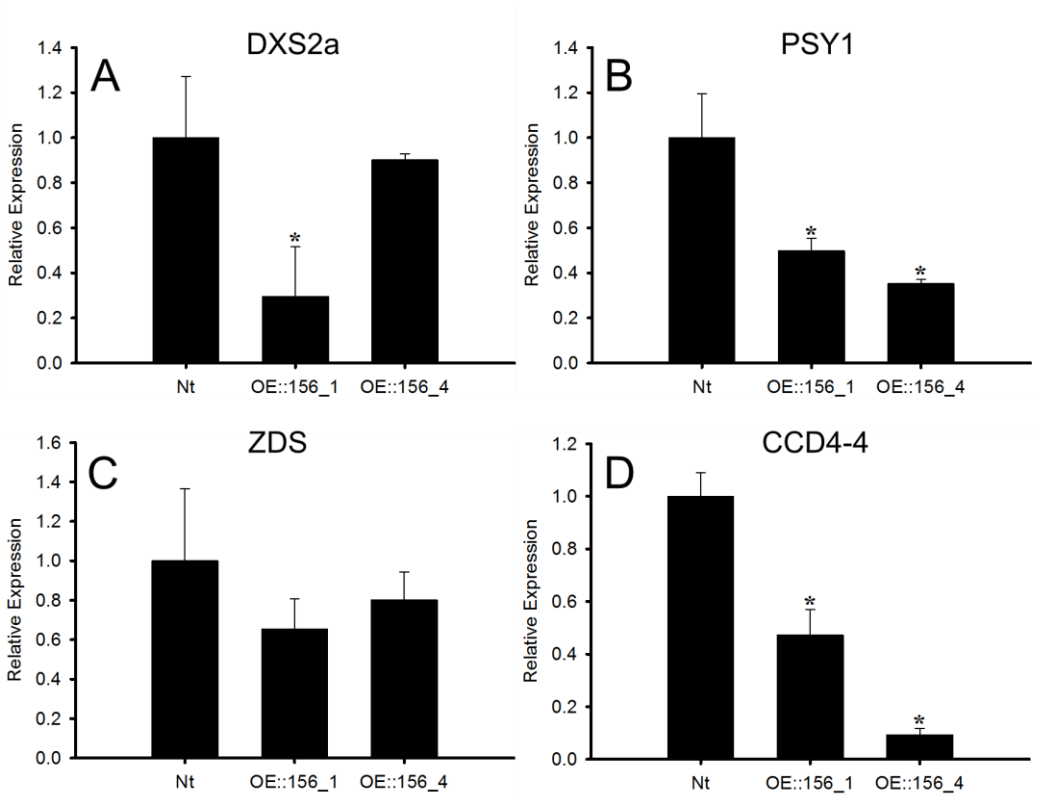

Figure 9. Relative expression levels of genes involved in carotenoid biosynthetic pathway *B. orellana* plants at 90th day grown in greenhouse. **A** - 1-deoxy-D-xylose-5-phosphate synthase 2a (DXS2a); **B** - Phytoene synthase 1 (PSY1); **C** - Zeta-carotene desaturase (ZDS); **D** - Carotenoid cleavage dioxygenase 4 (CCD4-4). Nt = Non-transformed, OE::156_1 = Plants overexpressing

miR156 line 1. OE::156_4 = Plants overexpressing miR156 line 4. Asterisks stand for *P*-value ≤ 0.05 using student-t test. Vertical bars correspond to standard error variation.

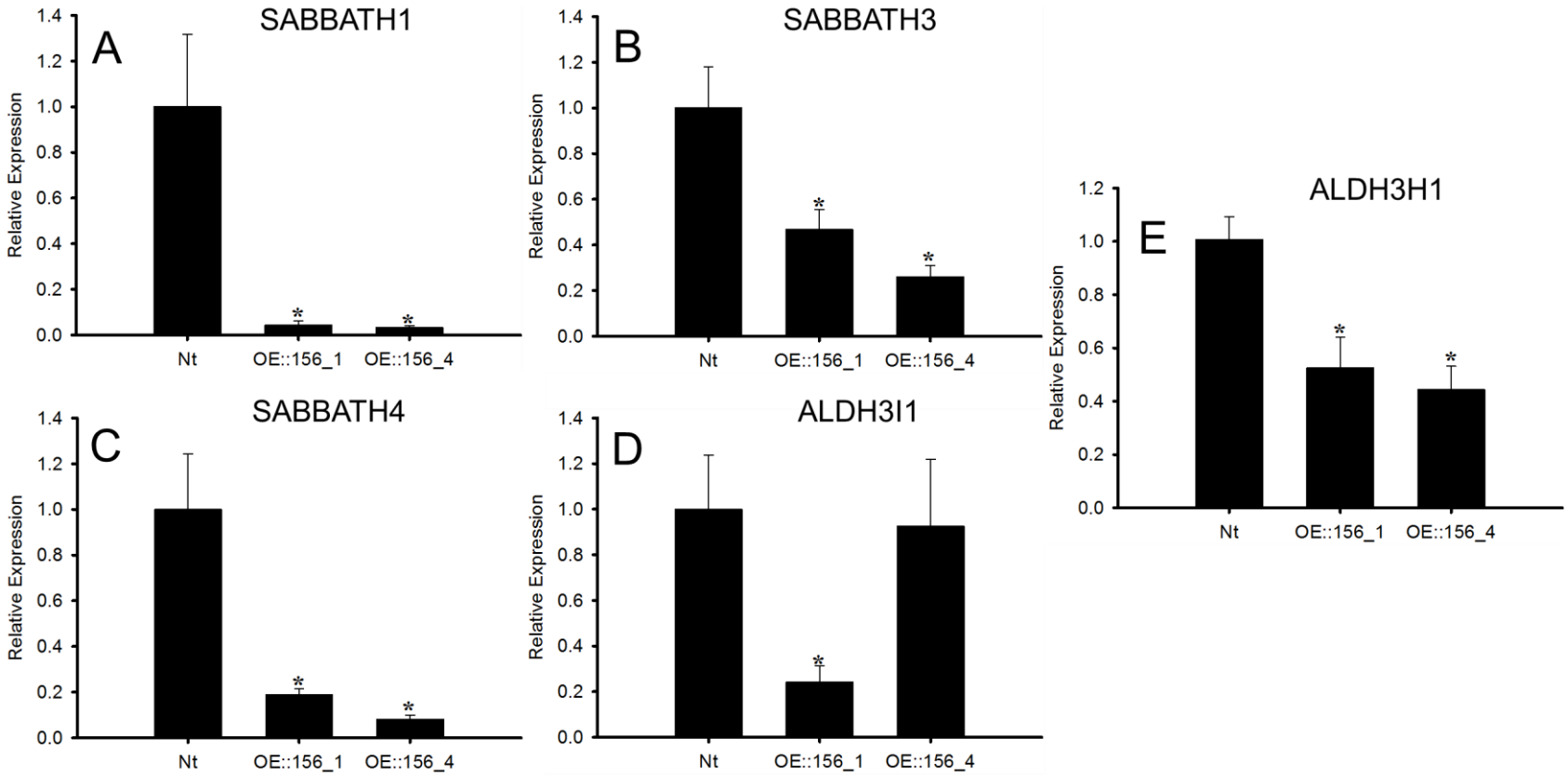

Figure 10. Expression levels of four bixin-related genes in *B. orellana* plants at the 90th of growth in greenhouse. **A** - SABBATH 1 ; **B** - SABBATH 3; **C** - SABBATH 4; **D** - Aldehyde dehydrogenase family 3 member I1 (ALDH3I1); **E** - Aldehyde dehydrogenase family 3 member H1 (ALDH3H1). Nt = Non-transformed, OE::156_1 = Plants overexpressing miR156 line 1. OE::156_4 = Plants

overexpressing miR156 line 4. Asterisks stands for *P*-value ≤ 0.05 using student-t test. Vertical bars correspond to standard error variation.

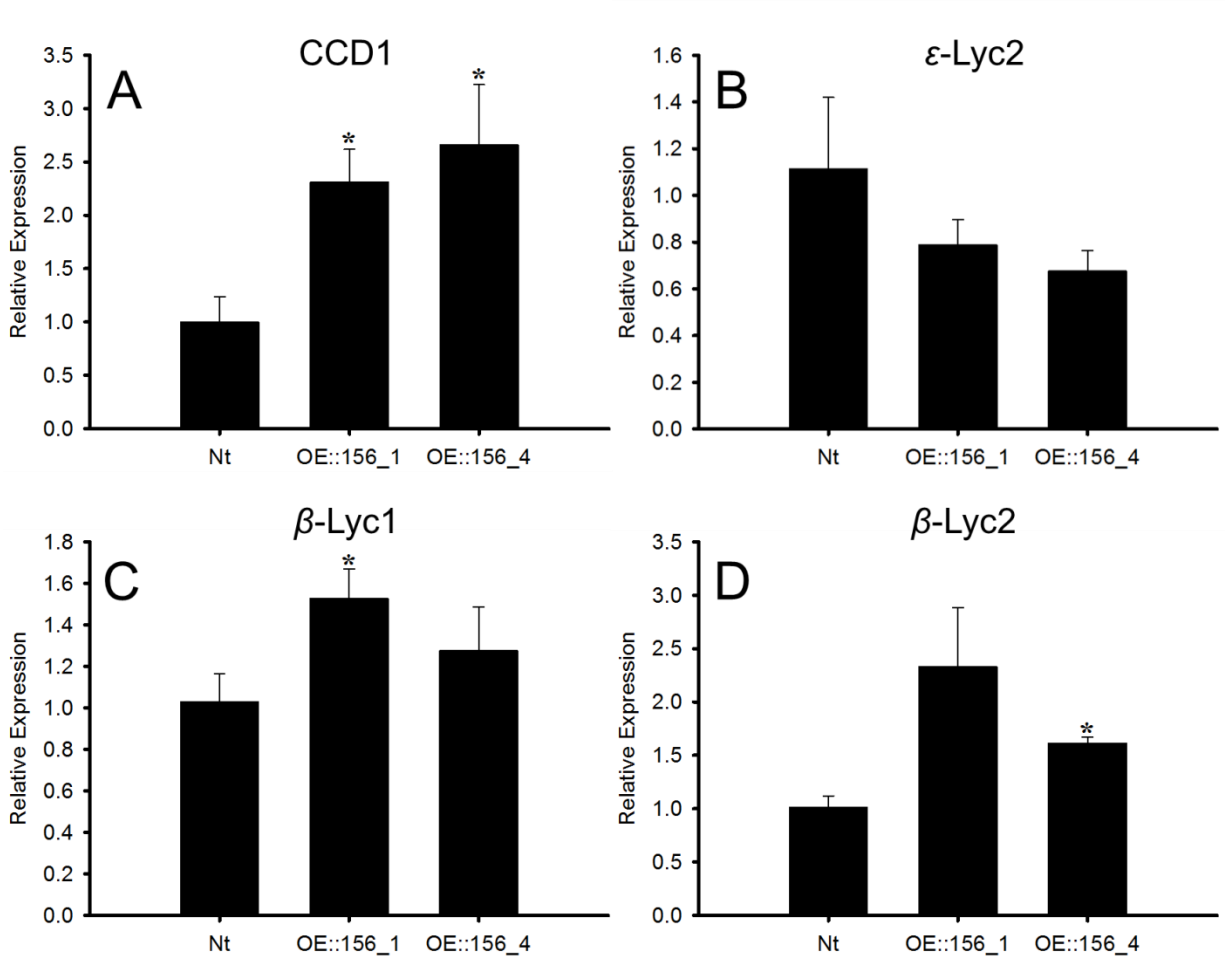

Figure 11. Expression levels of lycopene-related biosynthetic pathway in *B. orellana* plants at 90th day grown in greenhouse **A** - Carotenoid cleavage dioxygenase 1 (*CCD1*); **B** - Lycopene *ε*-cyclase 2 (*ε*-Lyc2); **C** - Lycopene *β*-cyclase 1 (*β*-Lyc1); **D** - Lycopene *β*-cyclase 2 (*β*-Lyc2). Nt = Non-transformed, OE::156_1 = Plants overexpressing miR156 line 1. OE::156_4 = Plants overexpressing miR156 line 4. Asterisks stands for *P*-value ≤ 0.05 using student-t test. Vertical bars correspond to standard error variation.

3.6 OE::156 line diverge its protein pools.

Since we aimed to understand how the module miR156/SPL changes OE::156 *B. orellana* plants secondary metabolism, we quantified and qualified the proteome of OE::156_4 line and relativized by Nt proteomics through mass spectrophotometry (Supplementary Table 1). This procedure helped numerous understandings of plant metabolism, from maize mechanism related to pathogen tolerance and resistance (Wang et al. 2019c) to the understanding of which medicinal plants are effective against Alzheimer's, depression, and schizophrenia diseases (Gonulalan et al. 2020).

Here, we observed 255 proteins with differential regulation in the plants with low levels of SPL active proteins (OE::156). Among them, 89 proteins were upaccumulated and 159 downaccumulated. When we looked for biological process relation (Supplementary table 1), about 6% of downaccumulated proteins were related to the cell cycle, as for example the protein tubulin beta-1 chain, the major component of beta-tubulin (Bassel et al. 2008). The miR156/SPL module also altered this group of proteins in the citrus callus, where somatic embryogenesis is the main metabolic process. This result was unexpected because OE::156_4 explants seems to have more regenerative power than Nt explants (Faria et al. 2021). Other GO-related categories also displayed the same pattern as showed in Cellular component biogenesis; Developmental processes; Cellular component organization; among others. This downaccumulation could be linked to the sampled organ. Inasmuch as we collected fully expanded leaves to understand the proteomic profile of OE::156 *B. orellana* plants.

Since, most proteins were downacumulated in OE::156 leaves (Figure 12) with few exceptions, as the enzyme superoxide dismutase, which is responsible for high ABA levels, a feature that was observed in OE::156 plants (Figure 5D). The same pattern was observed in *Nicotiana tabacum* (Zhang et al. 2008) and *Fagopyrum esculentum* (Salazar-Chavarría et al. 2020). In this way, we proceed analyzing which category these up and downaccumulated proteins are. We generated a KEGG pathway to separate each category of differently accumulated protein (Figure 13). Astonishingly, most proteins related to amino sugar and nucleotide metabolism, biosynthesis of amino acids, secondary metabolites biogenesis, and ribosome proteins

were downaccumulated. These proteins are involved in both primary and secondary metabolism pathways and could be regulated directly or indirectly by miR156/SPL module.

In the Gene Otology (GO) analysis (Suplmentary table 1), about 6% of downaccumulated proteins were related to the cell cycle, as for example the protein tubulin beta-1 chain, the major component of beta-tubulin (Bassel et al. 2008). The miR156/SPL module also altered this group of proteins in the citrus callus, where somatic embryogenesis is the main metabolic process. This result was unexpected because OE::156_4 explants have more regenerative power than Nt explants (Faria et al. 2021). Other GO-related categories also displayed the same pattern as showed in Cellular component biogenesis; Developmental processes; Cellular component organization; among others. This downaccumulation could be linked to the sampled organ. Inasmuch as we collected fully expanded leaves to understand the proteomic profile of OE::156 *B. orellana* plants.

Protein levels are good indication of gene and metabolic expression levels because avoid post-transcriptional regulation, which can deceive results reading or cause confusion about how pathways are responding to stimulus or regulation routes. We observed that most protein related to the biosynthesis of secondary metabolites are downaccumulated, and would be interesting to explore more, which routes are being affected by mir156/SPL module. Considering it, we use the proteomic data to select secondary metabolite-related proteins (Figure 14). This graphic shows that proteins related to, flavonoid, anthocyanin, lignin, and others were the most affected by our studied module in a manner to see patterns in, related proteins.

To explore more, we generated a volcano graphic with five highlighted important enzymes linked with these routes (Figure 15). The upaccumulated interesting enzyme is the zeaxanthin epoxidase (ZEP), which catalyzes the interconversions between the carotenoids and xanthines (Hieber et al. 2000). This enzyme is crucial for the ABA biosynthesis pathway (Marin et al. 1996). Even though, a new study suggests an ABA biosynthesis route that is ZEP independent, where ABA biosynthesis would start from other *β*-carotenoids and 9-cis-Zeaxanthin (Jia et al. 2022). Nevertheless, the upaccumulation of ZEP demonstrated that the carbons, which once would be going to bixin production, are now being employed in ABA biogenesis.

Flavonoids are a group of molecules with variable phenolic structures that has functions from growth to defense against pathogens, as well revised by Panche et al. (2016). The sulfotransferases enzymes, such as flavonol sulfotransferase, are responsible for bacteria defense, inducible by jasmonate and salicylic acid in Arabidopsis (Lacomme and Roby 1996). Furthermore, in Chinese cabbage (*Brassica rapa* L.), was observed flavonol sulfotransferases responsive to drought, salinity, and ABA as well (Jin et al. 2019). Moreover, in the genus *Gossypium*, members of the order Malvales, the same of *B. orellana*, the flavonol sulfotransferases are highly linked to fiber synthesis and trichome formation in different stages of plant development (Wang et al. 2019b). Otherwise, in *B. orellana* OE::156 plants, this enzyme is downaccumulated, since juvenile organs have fewer fibers and differentiated structures as trichomes or secondary cell walls.

Phenylalanine ammonia-lyase (PAL) is related to phenolic biosynthesis in higher plants. Since it is involved in the first step of the phenylpropanoid pathway. Hence, this enzyme deal with a noteworthy fixed carbon by the plant (Zhang and Liu 2015). In *Brachypodium*, defective PAL resulted in 43% less lignin, affecting plant growth and development, by reducing the amount of carbon used in the phenylpropanoid biogenesis route (Cass et al. 2015). Moreover, in rice, mutations of distinguishing PAL genes caused susceptibility to three different diseases caused by *fungi* (Tonnessen et al. 2015). Thus, PAL activity is linked to a series of plant metabolites, which implicate in plant growth and tolerance to environmental stresses, including *fungi* and drought response. That could explain why OE::156_4 plants do not have a carbon shortage for such expressive vegetative growth (Figure 1A) or enormous branching ratio (Figure 2C). Such evidence can also apply to how *B. orellana* miR156 overexpressing plants will deal with abiotic stresses in further works.

In this work, we quantified the anthocyanin total content in Nt and OE::156 plants (Table 2). We did not observe any total anthocyanin changes between the three lines used in these experiments. However, anthocyanin is a large group of different molecules and functions. Nevertheless, anthocyanin can have roles as excessive light protector, antioxidant, metal-chelating, and even in senescence process due to nutrition deficit (Landi et al. 2015). In tomato, anthocyanin completely defective mutants showed accumulation of reactive oxidative species and constitutive activation of defense responses under cold conditions (Qiu et al. 2016). Here we spotlight two

anthocyanin-related key enzymes: Anthocyanidin 3-O-glucosyltransferase and Anthocyanidin synthase. The first is responsible to convert anthocyanidin, a pigment that confers blue tonality to petals (Kazuma et al. 2004), into delphinidin, an anthocyanin (Hiromoto et al. 2015). On the other hand, the second has the function of synthesizing anthocyanidin from leucoanthocyanidin. This enzyme was accountable for almost double anthocyanin production in strawberry (*Fragaria* x *ananassa* Duch.) (Giampieri et al. 2018). Considering these results, the OE::156 plants display less potential in ROS and excessive light protection than the Nt type, since juvenelized plants displayed low light adaptation as seen in poplar (Lawrence et al. 2022). Such results suggest that overexpressing of miR156 could be more sensitive to sunstroke, which can be tested in future works.

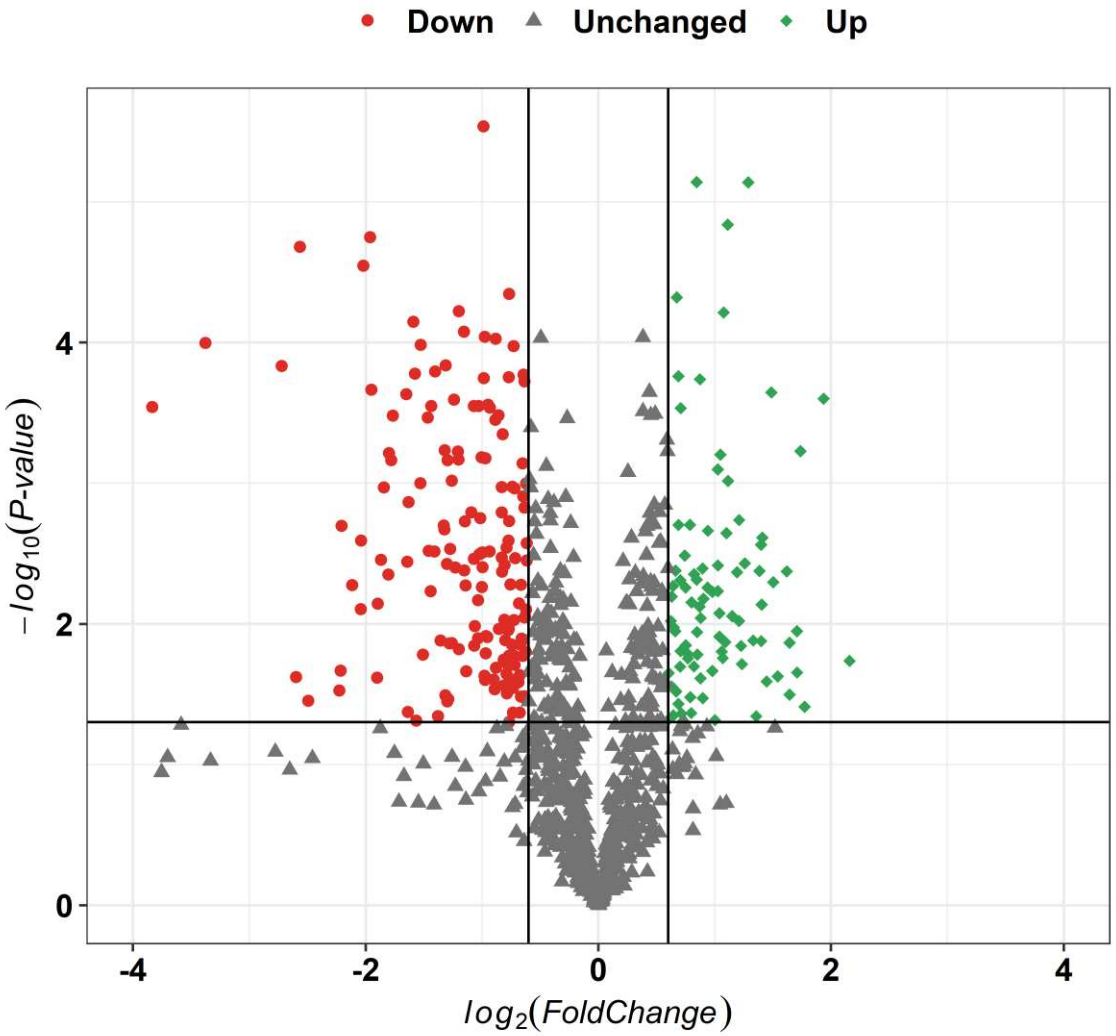

Figure 12. Volcano plot of the entire set of proteins quantified. Each point represents the difference in expression (fold-change) between a transgenic overexpressing line (OE::156_4) and non-transformed (Nt) annatto plants plotted against the level of statistical significance. Red dots: Downregulated proteins; Gray dots: Unchanged proteins; Green dots: Upregulated proteins.

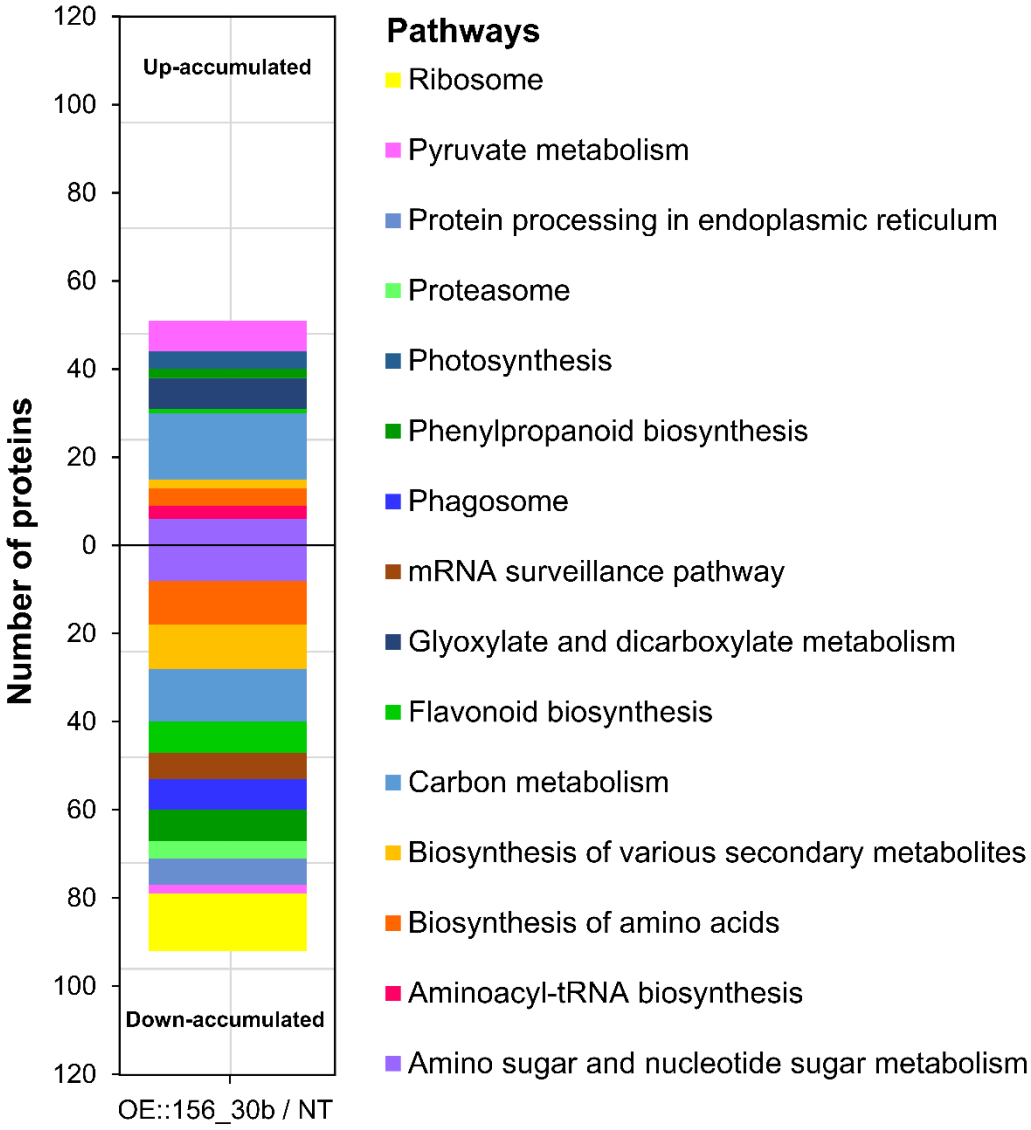

Figure 13. KEGG pathway enrichment analysis ($P \leq 0.01$) of differentially accumulated proteins (DAPs) identified from the OE::156_4 / Nt comparison. .

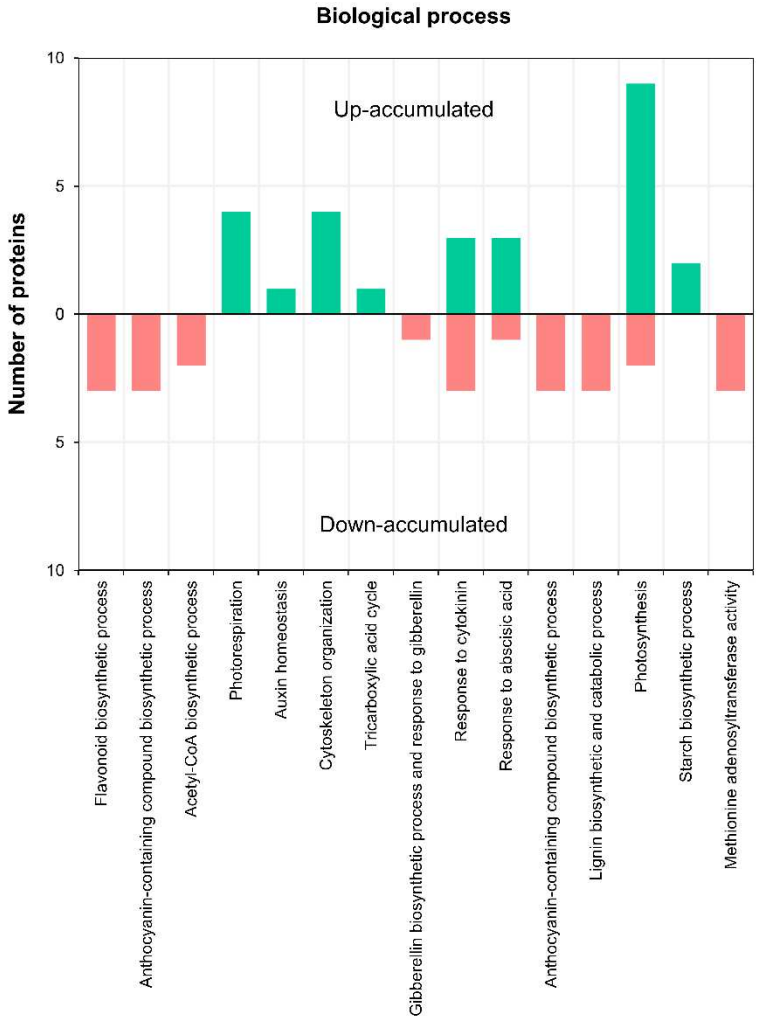

Figure 14. Functional annotation related to DAPs. Biological processes were enriched via Fisher's exact test with p-value 0.01, comparing differentially accumulated proteins in the OE::156_4/ Nt lines.

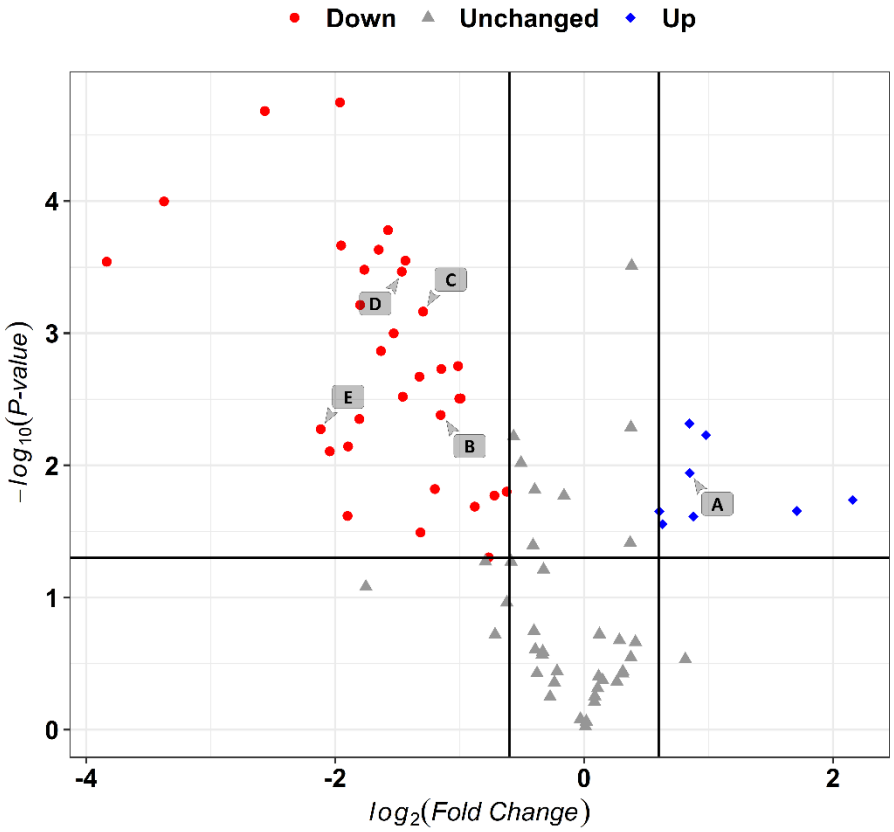

Figure 15. Volcano plot of secondary metabolism related proteins quantified. Each point represents the difference in expression (fold-change) between a transgenic overexpressing line (OE::156_4) and non-transformed (Nt) annatto plants plotted against the level of statistical significance. Red dots: Downaccumulated proteins; Gray dots: Unchanged proteins; Blue dots: Upregulated proteins; **A**: Zeaxanthin epoxidase; **B**: Flavonol sulfotransferase-like; **C**: Phenylalanine ammonia-lyase; **D**: Anthocyanidin 3-O-glucosyltransferase 5-like; **E**: Anthocyanidin synthase.

4. CONCLUSIONS AND PERSPECTIVES

The miR156/SPL module is well studied in numerous species and is well conserved in the higher plants group. However, the controlling nuances in different metabolites and developmental features are still under discussion. Here we illustrated one of this thin control in a species that have its studies only in the beginning: *Bixa orellana*.

Here, we were able to describe how these woody shrubs develop under greenhouse conditions with miR156 overexpression. The plants completely changed their leaf structure, without messing with the total leaf area; architecture, and grew its branches indefinitely. In addition, we were capable to understand how this growth was modulated, directly and indirectly, by changes in hormone profile under SPL deficiency. We observed that auxin might have accumulated OE::156 plants in the different organs, mainly because of the lack of the action of PIN proteins. Besides, we were able to see higher ABA levels in OE::156 plants, intriguing new questions about the natural dye biosynthesis pathway: bixin. Impressively, we encountered lower levels of bixin production in our transgenic, which led to new perceptions on carbon translocation among biosynthetic routes.

As revealed by RT-qPCR analyzes, we could posit a new carbon sink in *B. orellana* juvenilized plants, which once would allocate its photoassimilates mainly in bixin biosynthesis from the first days of its life cycle. In this analysis, CCD4 is downregulated and seems to be a key enzyme to lycopene changing in bixin aldehyde. Consequently, the enzymes SABBATHs also were downregulated, turning the carbon destination, which once would go to bixin production, unknown. Through the same technique, we were able to glimpse the first steps of carbon translocation. The CCD1 higher expression levels in OE::156 plants showed the first evidence. Then, *Lycopene β-cyclase* genes confirmed the xanthin pathway was the carbon sink we were looking for. All these results are summed up in the Figure 16.

To seize any gaps, the proteomics showed the upaccumulation of the ZEP enzyme, turning our understanding even more reliable. Besides that, from the proteomic results, we can ask new questions: How miR156 overexpressing plants will respond to drought? How is the root growth dynamics in these plants? Are miR156

overexpressing plants more likely to succumb under high irradiance? Just to mention a few.

This work provides new glimpses on how miR156/SPL module directly and indirectly rules other metabolic and physiological processes in woody plants. Here we show that the main metabolically changes were related to bixin biosynthesis and other secondary metabolites connected to plant adaptation to new edaphoclimatic scenarios and even biotic stresses.

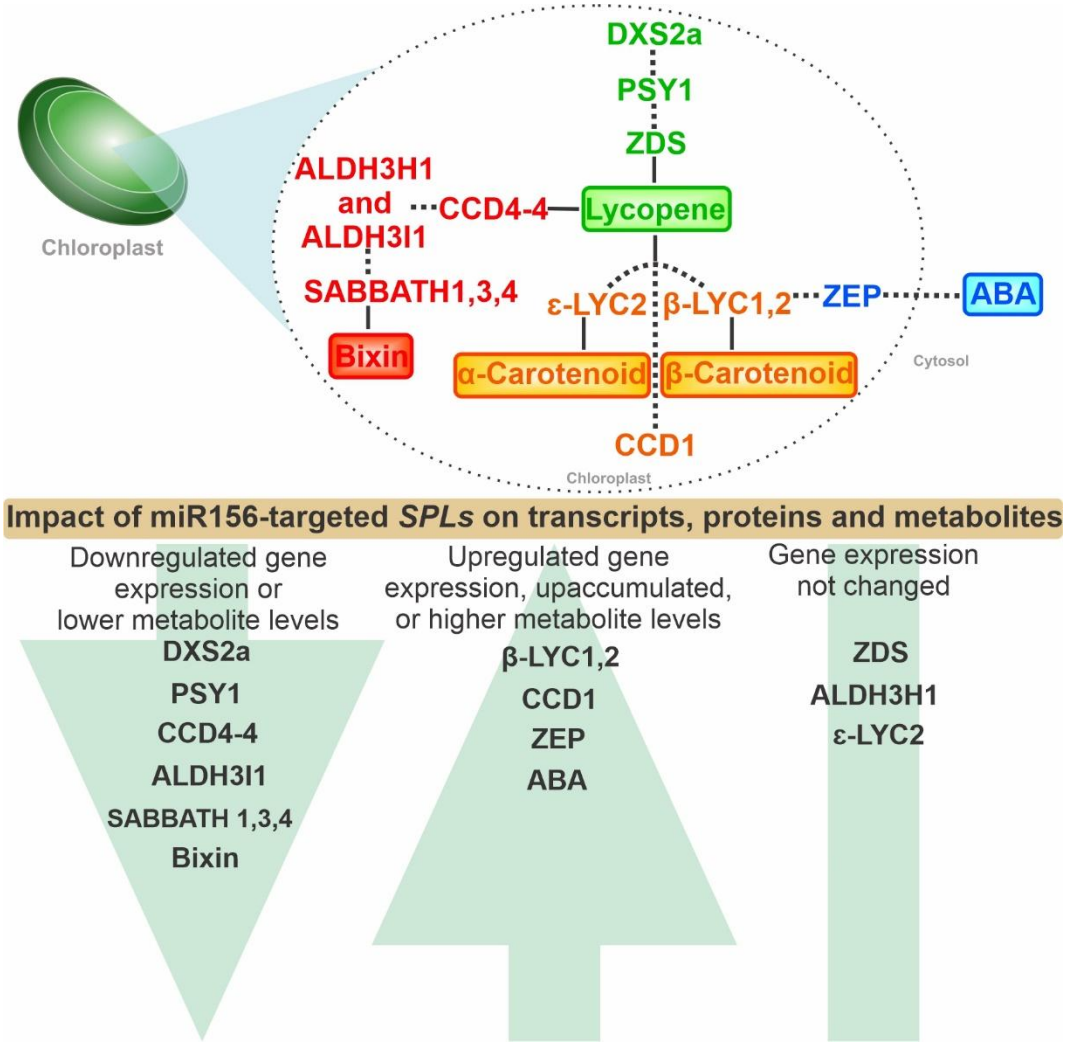
DXS2a
PSY1
ZDS
ALDH3H1
and
ALDH3I1
CCD4-4
Lycopene
Chloroplast
SABBATH1,3,4
ε-LYC2
β-LYC1,2
ZEP
ABA
Bixin
α-Carotenoid
β-Carotenoid
Cytosol
CCD1
Chloroplast
Impact of miR156-targeted SPLs on transcripts, proteins and metabolites
Downregulated gene expression or lower metabolite levels
DXS2a
PSY1
CCD4-4
ALDH3I1
SABBATH 1,3,4
Bixin
Upregulated gene expression, upaccumulated, or higher metabolite levels
β-LYC1,2
CCD1
ZEP
ABA
Gene expression not changed
ZDS
ALDH3H1
ε-LYC2

Figure 16. General view of carotenoid-related transcripts, proteins and metabolites changed by the miR156/SPL module in *B. orellana* plants overexpressing miR156 (OE::156). Dotted line = indirectly in the route; Continuous line = directly related in the metabolic pathway.

5. REFERENCES

Almeida AL, Freitas PF de, Ferreira CP, Ventrella MC (2021) Syncytial development of annatto (*Bixa orellana* L.) pigment gland: A curious type of anastomosed articulated laticifer. Flora Morphol Distrib Funct Ecol Plants 274: https://doi.org/10.1016/j.flora.2020.151727.

Anwar A, Liu Y, Dong R, Bai L, Yu X, Li Y (2018) The physiological and molecular mechanism of brassinosteroid in response to stress: A review. Biol Res 51:1–15. https://doi.org/10.1186/s40659-018-0195-2

Arshad M, Feyissa BA, Amyot L, Aung B, Hannoufa A (2017) MicroRNA156 improves drought stress tolerance in alfalfa (*Medicago sativa*) by silencing SPL13. Plant Sci 258:122–136. https://doi.org/10.1016/j.plantsci.2017.01.018

Avni A, Bailey BA, Mattoo AK, Anderson JD (1994) Induction of ethylene biosynthesis in Nicotiana tabacum by a Trichoderma viride xylanase is correlated to the accumulation of 1-aminocyclopropane-1-carboxylic acid (ACC) synthase and ACC oxidase transcripts. Plant Physiol 106:1049–1055. https://doi.org/10.1104/pp.106.3.1049

Baliane A (1982) Cultura do urucueiro. Rio de Janeiro: Empresa de Assistência Técnica e Extensão Rural (EMATER-Rio).

Barbier FF, Dun EA, Beveridge CA (2017) Apical dominance. Curr Biol 27:R864–R865. https://doi.org/10.1016/j.cub.2017.05.024

Barrera-Rojas CH, Rocha GHB, Polverari L, Pinheiro Brito DiA, Batista DiS, Notini MM, Da Cruz ACF, Morea EGO, Sabatini S, Otoni WC, Nogueira FTS (2020) MiR156-targeted SPL10 controls Arabidopsis root meristem activity and root-derived de novo shoot regeneration via cytokinin responses. J Exp Bot 71:934–950. https://doi.org/10.1093/jxb/erz475

Bassel GW, Fung P, Chow TFF, Foong JA, Provart NJ, Cutler SR (2008) Elucidating the germination transcriptional program using small molecules. Plant Physiol 147:143–155. https://doi.org/10.1104/pp.107.110841

Baumberger N, Baulcombe DC (2005) Arabidopsis ARGONAUTE1 is an RNA Slicer that selectively recruits microRNAs and short interfering RNAs. Proc Natl Acad Sci U S A 102:11928–11933. https://doi.org/10.1073/pnas.0505461102

Bentley BL (1977) The Protective Function of Ants Visiting the Extrafloral Nectaries of

Bixa orellana. J Ecol 65:27–38. https://doi.org/10.2307/2259060

Bhogale S, Mahajan AS, Natarajan B, Rajabhoj M, Thulasiram H V., Banerjee AK (2014) MicroRNA156: A potential graft-transmissible microrna that modulates plant architecture and tuberization in *Solanum tuberosum* ssp. andigena. Plant Physiol 164:1011–1027. https://doi.org/10.1104/pp.113.230714

Bollman KM, Aukerman MJ, Park MY, Hunter C, Berardini TZ, Scott Poethig R (2003) HASTY, the Arabidopsis ortholog of exportin 5/MSN5, regulates phase change and morphogenesis. Development 130:1493–1504. https://doi.org/10.1242/dev.00362

Bologna NG, Iselin R, Abriata LA, Sarazin A, Pumplin N, Jay F, Grentzinger T, Dal Peraro M, Voinnet O (2018) Nucleo-cytosolic Shuttling of ARGONAUTE1 Prompts a Revised Model of the Plant MicroRNA Pathway. Mol Cell 69:709–719.e5. https://doi.org/10.1016/j.molcel.2018.01.007

Brasileiro M and C Carneiro (2015) Manual de transformação genética de plantas, 2ª Edição revisada e ampliada, Embrapa-SPI/Embrapa-Cenargen, Brasília.

Brocker C, Vasiliou M, Carpenter S, Carpenter C, Zhang Y, Wang X, Kotchoni SO, Wood AJ, Kirch HH, Kopečný D, Nebert DW, Vasiliou V (2013) Aldehyde dehydrogenase (ALDH) superfamily in plants: Gene nomenclature and comparative genomics. Planta 237:189–210. https://doi.org/10.1007/s00425-012-1749-0

Cárdenas-Conejo Y, Carballo-Uicab V, Lieberman M, Aguilar-Espinosa M, Comai L, Rivera-Madrid R (2015) De novo transcriptome sequencing in *Bixa orellana* to identify genes involved in methylerythritol phosphate, carotenoid and bixin biosynthesis. BMC Genomics 16:. https://doi.org/10.1186/s12864-015-2065-4

Cardon G, Höhmann S, Klein J, Nettesheim K, Saedler H, Huijser P (1999) Molecular characterisation of the Arabidopsis SBP-box genes. Gene 237:91–104. https://doi.org/10.1016/S0378-1119(99)00308-X

Cass CL, Peraldi A, Dowd PF, et al (2015) Effects of PHENYLALANINE AMMONIA LYASE (PAL) knockdown on cell wall composition, biomass digestibility, and biotic and abiotic stress responses in Brachypodium. J Exp Bot 66:4317–4335. https://doi.org/10.1093/jxb/erv269

Cazzonelli CI, Pogson BJ (2010) Source to sink: regulation of carotenoid biosynthesis in plants. Trends Plant Sci 15:266–274.

https://doi.org/10.1016/j.tplants.2010.02.003

Chen K, Li GJ, Bressan RA, Song CP, Zhu JK, Zhao Y (2020) Abscisic acid dynamics, signaling, and functions in plants. J Integr Plant Biol 62:25–54. https://doi.org/10.1111/jipb.12899

Cheong JJ, Choi Y Do (2003) Methyl jasmonate as a vital substance in plants. Trends Genet 19:409–413. https://doi.org/10.1016/S0168-9525(03)00138-0

Coll Y, Coll F, Amorós A, Pujol M (2015) Brassinosteroids roles and applications: An up-date. Biol 70:726–732. https://doi.org/10.1515/biolog-2015-0085

Conesa A, Götz S, García-Gómez JM, Terol J, Talón M, Robles M (2005) Blast2GO: A universal tool for annotation, visualization and analysis in functional genomics research. Bioinformatics 21:3674–3676. https://doi.org/10.1093/bioinformatics/bti610

Cui LG, Shan JX, Shi M, Gao JP, Lin HX (2014) The miR156-SPL9-DFR pathway coordinates the relationship between development and abiotic stress tolerance in plants. Plant J 80:1108–1117. https://doi.org/10.1111/tpj.12712

Dai Z, Wang J, Yang X, Lu H, Miao X, Shi Z (2018) Modulation of plant architecture by the miR156f-OsSPL7-OsGH3.8 pathway in rice. J Exp Bot 69:5117–5130. https://doi.org/10.1093/jxb/ery273

Das PK, Shin DH, Choi SB, Park Y Il (2012) Sugar-hormone cross-talk in anthocyanin biosynthesis. Mol Cells 34:501–507. https://doi.org/10.1007/s10059-012-0151-x

Distler U, Kuharev J, Navarro P, Levin Y, Schild H, Tenzer S (2014) Drift time-specific collision energies enable deep-coverage data-independent acquisition proteomics. Nat Methods 11:167–170. https://doi.org/10.1038/nmeth.2767

Fahlgren N, Howell MD, Kasschau KD, Chapman EJ, Sullivan CM, Cumbie JS, Givan SA, Law TF, Grant SR, Dangl JL, Carrington JC (2007) High-throughput sequencing of Arabidopsis microRNAs: Evidence for frequent birth and death of MIRNA genes. PLoS One 2:. https://doi.org/10.1371/journal.pone.0000219

Fang L, Wang Y, Sederoff RR (2021) MicroRNAs in Woody Plants. 12:1–17. https://doi.org/10.3389/fpls.2021.686831

Faria DV, Correia LN de F, Souza MVC, Ríos-Ríos AM, Vital CE, Batista DS, Costa MGC, Otoni WC (2019a) Irradiance and light quality affect two annatto (*Bixa orellana* L.) cultivars with contrasting bixin production. J Photochem Photobiol B Biol 197:111549. https://doi.org/10.1016/j.jphotobiol.2019.111549

Faria DV, de Freitas Correia LN, Batista DS, Vital CE, Heringer AS, De-la-Peña C, Costa MGC, Guerra MP, Otoni WC (2020) 5-Azacytidine downregulates the SABATH methyltransferase genes and augments bixin content in *Bixa orellana* L. leaves. Plant Cell Tissue Organ Cult 142:425–434. https://doi.org/10.1007/s11240-020-01857-8

Faria DV, de Freitas Correia LN, de Matos EM, de Souza MVC, Batista DS, Costa MGC, de Paiva Neto VB, Xavier A, Rogalski M, Otoni WC (2019b) Wounding and medium formulation affect de novo shoot organogenic responses in hypocotyl-derived explants of annatto (*Bixa orellana* L.). Vitr Cell Dev Biol - Plant 55:277–289. https://doi.org/10.1007/s11627-019-09978-2

Faria DV, Freitas DMS, Duarte MBS, Machado KL de G, Matos EM, Batista DS, Costa MGC, Viccini LF, Nogueira FTS, Otoni WC (2021) Agrobacterium - mediated transformation of annatto (*Bixa orellana* L.): protocol optimization and overexpression of microRNA 156 in transgenic plants. Plant Cell, Tissue Organ Cult. https://doi.org/10.1007/s11240-021-02211-2

Feng S, Xu Y, Guo C, Zheng J, Zhou B, Zhang Y, Ding Y, Zhang L, Zhu Z, Wang H, Wu G (2016) Modulation of miR156 to identify traits associated with vegetative phase change in tobacco (*Nicotiana tabacum*). J Exp Bot 67:1493–1504. https://doi.org/10.1093/jxb/erv551

Feyissa BA, Arshad M, Gruber MY, Kohalmi SE, Hannoufa A (2019) The interplay between miR156/SPL13 and DFR/WD40-1 regulate drought tolerance in alfalfa. BMC Plant Biol 19:1–19. https://doi.org/10.1186/s12870-019-2059-5

Feyissa BA, Renaud J, Nasrollahi V, Kohalmi SE, Hannoufa A (2020) Transcriptome-IPMS analysis reveals a tissue-dependent miR156/SPL13 regulatory mechanism in alfalfa drought tolerance. BMC Genomics 21:1–18. https://doi.org/10.1186/s12864-020-07118-4

Finkelstein R (2013) Abscisic Acid Synthesis and Response. Arab B 11:e0166. https://doi.org/10.1199/tab.0166

Fouracre JP, Poethig RS (2016) The role of small RNAs in vegetative shoot development. Curr Opin Plant Biol 29:64–72. https://doi.org/10.1016/j.pbi.2015.11.006

Fouracre JP, Poethig SR (2019) Role for the shoot apical meristem in the specification of juvenile leaf identity in Arabidopsis. Proc Natl Acad Sci U S A 116:10168–

10177. https://doi.org/10.1073/pnas.1817853116

Fouracre JP, Scott Poethig R (2019) Role for the shoot apical meristem in the specification of juvenile leaf identity in Arabidopsis. Proc Natl Acad Sci U S A 116:10168–10177. https://doi.org/10.1073/pnas.1817853116

Fu X, Feng C, Wang C, Yin X, Lu P, Grierson D, Xu C, Chen K (2014) Involvement of multiple phytoene synthase genes in tissue-and cultivar-specific accumulation of carotenoids in loquat. J Exp Bot 65:4679–4689. https://doi.org/10.1093/jxb/eru257

Gajdošová S, Spíchal L, Kamínek M, et al (2011) Distribution, biological activities, metabolism, and the conceivable function of cis-zeatin-type cytokinins in plants. J Exp Bot 62:2827–2840. https://doi.org/10.1093/jxb/erq457

Giampieri F, Gasparrini M, Forbes-Hernandez TY, et al (2018) Overexpression of the Anthocyanidin Synthase Gene in Strawberry Enhances Antioxidant Capacity and Cytotoxic Effects on Human Hepatic Cancer Cells. J Agric Food Chem 66:581–592. https://doi.org/10.1021/acs.jafc.7b04177

Giuliano G, Rosati C, Bramley PM (2003) To dye or not to dye: Biochemistry of annatto unveiled. Trends Biotechnol 21:513–516. https://doi.org/10.1016/j.tibtech.2003.10.001

Gonulalan EM, Nemutlu E, Bayazeid O, Koçak E, Yalçın FN, Demirezer LO (2020) Metabolomics and proteomics profiles of some medicinal plants and correlation with BDNF activity. Phytomedicine 74:152920. https://doi.org/10.1016/j.phymed.2019.152920

Gou J, Fu C, Liu S, Tang C, Debnath S, Flanagan A, Ge Y, Tang Y, Jiang Q, Larson PR, Wen J, Wang ZY (2017) The miR156-SPL4 module predominantly regulates aerial axillary bud formation and controls shoot architecture. New Phytol. https://doi.org/10.1111/nph.14758

Gou JY, Felippes FF, Liu CJ, Weigel D, Wang JW (2011) Negative Regulation of Anthocyanin Biosynthesis in Arabidopsis by a miR156-Targeted SPL Transcription Factor. Plant Cell 23:1512–1522. https://doi.org/10.1105/tpc.111.084525

Grove MD, Spencer GF, Rohwedder WK, Mandava N, Worley JF, Warthen JD, Steffens GL, Flippen-Anderson JL, Cook JC (1979) Brassinolide, a plant growth-promoting steroid isolated from *Brassica napus* pollen. Nature 281:216–217

Guo Q, Li L, Zhao K, Yao W, Cheng Z, Zhou B, Jiang T (2021) Genome-wide analysis of poplar squamosa-promoter-binding protein (Sbp) family under salt stress.

Forests 12:. https://doi.org/10.3390/f12040413

Gupta R, Chakrabarty SK (2013) Gibberellic acid in plant: Still a mystery unresolved. Plant Signal Behav 8:. https://doi.org/10.4161/psb.25504

Hausser J, Zavolan M (2014) Identification and consequences of miRNA-target interactions-beyond repression of gene expression. Nat Rev Genet 15:599–612. https://doi.org/10.1038/nrg3765

Hieber AD, Bugos RC, Yamamoto HY (2000) Plant lipocalins: Violaxanthin de-epoxidase and zeaxanthin epoxidase. Biochim Biophys Acta - Protein Struct Mol Enzymol 1482:84–91. https://doi.org/10.1016/S0167-4838(00)00141-2

Hiromoto T, Honjo E, Noda N, Tamada T, Kazuma K, Suzuki M, Blaber M, Kuroki R (2015) Structural basis for acceptor-substrate recognition of UDP-glucose: Anthocyanidin 3-O-glucosyltransferase from *Clitoria ternatea*. Protein Sci 24:395–407. https://doi.org/10.1002/pro.2630

Hu Y, Xie Q, Chua NH (2003) The Arabidopsis auxin-inducible gene ARGOS controls lateral organ size. Plant Cell 15:1951–1961. https://doi.org/10.1105/tpc.013557

Ito T, Okada K, Fukazawa J, Takahashi Y (2018) DELLA-dependent and -independent gibberellin signaling. Plant Signal Behav 13:1–3. https://doi.org/10.1080/15592324.2018.1445933

Jia KP, Mi J, Ali S, Ohyanagi H, Moreno JC, Ablazov A, Balakrishna A, Berqdar L, Fiore A, Diretto G, Martínez C, de Lera AR, Gojobori T, Al-Babili S (2022) An alternative, zeaxanthin epoxidase-independent abscisic acid biosynthetic pathway in plants. Mol Plant 15:151–166. https://doi.org/10.1016/j.molp.2021.09.008

Jin L, Ouyang N, Huang Y, Liu C, Ruan Y (2019) Genome-wide analysis of sulfotransferase genes and their responses to abiotic stresses in Chinese cabbage (*Brassica rapa* L.). PLoS One 14:1–17. https://doi.org/10.1371/journal.pone.0221422

Johnson CR, Millwood RJ, Tang Y, Gou J, Sykes RW, Turner GB, Davis MF, Sang Y, Wang ZY, Stewart CN (2017) Field-grown miR156 transgenic switchgrass reproduction, yield, global gene expression analysis, and bioconfinement. Biotechnol Biofuels 10:1–12. https://doi.org/10.1186/s13068-017-0939-1

Jones-Rhoades MW, Bartel DP, Bartel B (2006) MicroRNAs and their regulatory roles in plants. Annu Rev Plant Biol 57:19–53. https://doi.org/10.1146/annurev.arplant.57.032905.105218

Jung JH, Ju Y, Seo PJ, Lee JH, Park CM (2012) The SOC1-SPL module integrates photoperiod and gibberellic acid signals to control flowering time in Arabidopsis. Plant J 69:577–588. https://doi.org/10.1111/j.1365-313X.2011.04813.x

Jung JH, Seo PJ, Kang SK, Park CM (2011) miR172 signals are incorporated into the miR156 signaling pathway at the SPL3/4/5 genes in Arabidopsis developmental transitions. Plant Mol Biol 76:35–45. https://doi.org/10.1007/s11103-011-9759-z

Karmakar UK, Sultana S, Nishi S, Biswas NN, Hossain L, Sheikh S (2018) Antioxidant, analgesic, antimicrobial, and anthelmintic activity of the dried seeds of *Bixa orellana* (L). Int J Pharm (Hyderabad, India) 8:150–163

Kaur N, Pandey A, Shivani, Kumar P, Pandey P, Kesarwani AK, Mantri SS, Awasthi P, Tiwari S (2017) Regulation of banana phytoene synthase (MaPSY) expression, characterization and their modulation under various abiotic stress conditions. Front Plant Sci 8:1–17. https://doi.org/10.3389/fpls.2017.00462

Kazuma K, Kogawa K, Noda N, Kato N, Suzuki M (2004) Identification of delphinidin 3-O-(6′-O-Malonyl)-β-glucoside- 3′-O-β-glucoside, a postulated intermediate in the biosynthesis of ternatin C5in the blue petals of *Clitoria ternatea* (butterfly pea). Chem Biodivers 1:1762–1770. https://doi.org/10.1002/cbdv.200490132

Kuluev BR, Knyazev A V., Mikhaylova E V., Ermoshin AA, Nikonorov YM, Chemeris A V. (2016) The poplar ARGOS-LIKE gene promotes leaf initiation and cell expansion, and controls organ size. Biol Plant 60:513–522. https://doi.org/10.1007/s10535-016-0610-x

Kurihara Y, Watanabe Y (2004) Arabidopsis micro-RNA biogenesis through Dicer-like 1 protein functions. Proc Natl Acad Sci U S A 101:12753–12758. https://doi.org/10.1073/pnas.0403115101

Lacomme C, Roby D (1996) Molecular cloning of a sulfotransferase in Arabidopsis thaliana and regulation during development and in response to infection with pathogenic bacteria. Plant Mol Biol 30:995–1008. https://doi.org/10.1007/BF00020810

Lacuesta M, Saiz-Fernández I, Podlešáková K, Miranda-Apodaca J, Novák O, Doležal K, De Diego N (2018) The trans and cis zeatin isomers play different roles in regulating growth inhibition induced by high nitrate concentrations in maize. Plant Growth Regul 85:199–209. https://doi.org/10.1007/s10725-018-0383-7

LaFountain AM, Yuan YW (2021) Repressors of anthocyanin biosynthesis. New Phytol

231:933–949. https://doi.org/10.1111/nph.17397

Landi M, Tattini M, Gould KS (2015) Multiple functional roles of anthocyanins in plant-environment interactions. Environ Exp Bot 119:4–17. https://doi.org/10.1016/j.envexpbot.2015.05.012

Lawrence EH, Leichty AR, Doody EE, Ma C, Strauss SH, Poethig RS (2021) Vegetative phase change in *Populus tremula* × *alba*. New Phytol 231:351–364. https://doi.org/10.1111/nph.17316

Lawrence EH, Leichty AR, Ma C, Strauss SH, Poethig SR (2020a) Vegetative phase change in Populus tremula x alba. biorxiv June:1–15

Lawrence EH, Springer CJ, Helliker BR, Poethig RS (2020b) miR156-mediated changes in leaf composition lead to altered photosynthetic traits during vegetative phase change. New Phytol nph.17007. https://doi.org/10.1111/nph.17007

Lawrence EH, Springer CJ, Helliker BR, Scott Poethig R (2022) The carbon economics of vegetative phase change. Plant Cell Environ. https://doi.org/10.1111/pce.14281

Leichty AR, Poethig SR (2019) Development and evolution of age-dependent defenses in ant-acacias. Proc Natl Acad Sci U S A 116:15596–15601. https://doi.org/10.1073/pnas.1900644116

Levy A, Szwerdszarf D, Abu-Abied M, Mordehaev I, Yaniv Y, Riov J, Arazi T, Sadot E (2014) Profiling microRNAs in Eucalyptus grandis reveals no mutual relationship between alterations in miR156 and miR172 expression and adventitious root induction during development. BMC Genomics 15:1–9. https://doi.org/10.1186/1471-2164-15-524

Liang YC, Reid MS, Jiang CZ (2014) Controlling plant architecture by manipulation of gibberellic acid signalling in petunia. Hortic Res 1:1–6. https://doi.org/10.1038/hortres.2014.61

Lin FF, Qiu LF, Deng JS, Shi YY, Chen LS, Wang K (2010) Investigation of SPAD meter-based indices for estimating rice nitrogen status. Comput Electron Agric 71:60–65. https://doi.org/10.1016/j.compag.2009.09.006

Liu H, Yu H, Tang G, Huang T (2018) Small but powerful: function of microRNAs in plant development. Plant Cell Rep 37:515–528. https://doi.org/10.1007/s00299-017-2246-5

Liu H, Zhang Y, Yang F, Qi X, Ahmad H, Wu C, Cheng Z (2019) Effect of the mode and time of gibberellic acid treatment on plant architecture and bulb structure in

garlic (*Allium sativum* L.). Sci Hortic (Amsterdam) 257:108723. https://doi.org/10.1016/j.scienta.2019.108723

Livak KJ, Schmittgen TD (2001) Analysis of Relative Gene Expression Data Using Real- Time Quantitative PCR and the 2^(-delta delta CT) Method. METHODS 28:402–408. https://doi.org/10.1006/meth.2001.1262

Llave C, Kasschau KD, Rector MA, Carrington JC (2002) Endogenous and silencing-associated small RNAs in plants. Plant Cell 14:1605–1619. https://doi.org/10.1105/tpc.003210

Long JM, Liu CY, Feng MQ, Liu Y, Wu XM, Guo WW (2018) MiR156-SPL modules regulate induction of somatic embryogenesis in citrus callus. J Exp Bot 69:2979–2993. https://doi.org/10.1093/jxb/ery132

Louro RP, Santiago LJM (2015) Development of carotenoid storage cells in Bixa orellana L. seed arils. Protoplasma 253:77–86. https://doi.org/10.1007/s00709-015-0789-2

Lucani CJ, Brodribb TJ, Jordan GJ, Mitchell PJ (2019) Juvenile and adult leaves of heteroblastic *Eucalyptus globulus* vary in xylem vulnerability. Trees - Struct Funct 33:1167–1178. https://doi.org/10.1007/s00468-019-01851-4

Mao YB, Liu YQ, Chen DY, Chen FY, Fang X, Hong GJ, Wang LJ, Wang JW, Chen XY (2017) Jasmonate response decay and defense metabolite accumulation contributes to age-regulated dynamics of plant insect resistance. Nat Commun 8:1–13. https://doi.org/10.1038/ncomms13925

Marin E, Nussaume L, Quesada A, Gonneau M, Sotta B, Hugueney P, Frey A, Marion-Poll A (1996) Molecular identification of zeaxanthin epoxidase of Nicotiana plumbaginifolia, a gene involved in abscisic acid biosynthesis and corresponding to the ABA locus of *Arabidopsis thaliana*. EMBO J 15:2331–2342. https://doi.org/10.1002/j.1460-2075.1996.tb00589.x

Mashiguchi K, Tanaka K, Sakai T, et al (2011) The main auxin biosynthesis pathway in Arabidopsis. Proc Natl Acad Sci U S A 108:18512–18517. https://doi.org/10.1073/pnas.1108434108

Miranda RM de, Nery LA, Ventrella MC (2017) Extrafloral nectaries of annatto (*Bixa orellana* L.): Anatomy, nectar composition and activity during organ development. Acta Bot Brasilica 31:468–476. https://doi.org/10.1590/0102-33062017abb0191

Moreira PA, Lins J, Dequigiovanni G, Veasey EA, Clement CR (2015) The

domestication of annatto (*Bixa orellana*) from *Bixa urucurana* in Amazonia. Econ Bot 69:127–135. https://doi.org/10.1007/s12231-015-9304-0

Morris SE, Turnbull CGN, Murfet IC, Beveridge CA (2001) Mutational analysis of branching in pea. Evidence that Rms1 and Rms5 regulate the same novel signal. Plant Physiol 126:1205–1213. https://doi.org/10.1104/pp.126.3.1205

Nanjo Y, Skultety L, Uváčková L, Klubicová K, Hajduch M, Komatsu S (2012) Mass spectrometry-based analysis of proteomic changes in the root tips of flooded soybean seedlings. J Proteome Res 11:372–385. https://doi.org/10.1021/pr200701y

Napoleão TA, Soares G, Vital CE, Bastos C, Castro R, Loureiro ME, Giordano A (2017) Methyl jasmonate and salicylic acid are able to modify cell wall but only salicylic acid alters biomass digestibility in the model grass Brachypodium distachyon. Plant Sci 263:46–54. https://doi.org/10.1016/j.plantsci.2017.06.014

Neff MM, Chory J (1998) Genetic interactions between phytochrome A, phytochrome B, and cryptochrome 1 during arabidopsis development. Plant Physiol 118:27–36. https://doi.org/10.1104/pp.118.1.27

Ohmiya A, Kishimoto S, Aida R, Yoshioka S, Sumitomo K (2006) Carotenoid cleavage dioxygenase (CmCCD4a) contributes to white color formation in Chrysanthemum petals. Plant Physiol 142:1193–1201. https://doi.org/10.1104/pp.106.087130

Osadchuk K, Cheng CL, Irish EE (2019) Jasmonic acid levels decline in advance of the transition to the adult phase in maize. Plant Direct 3:1–13. https://doi.org/10.1002/pld3.180

Panche AN, Diwan AD, Chandra SR (2016) Flavonoids: An overview. J Nutr Sci 5:. https://doi.org/10.1017/jns.2016.41

Park MY, Wu G, Gonzalez-Sulser A, Vaucheret H, Poethig RS (2005) Nuclear processing and export of microRNAs in Arabidopsis. Proc Natl Acad Sci U S A 102:3691–3696. https://doi.org/10.1073/pnas.0405570102

Poethig RS (2009) Small RNAs and developmental timing in plants. Curr Opin Genet Dev 19:374–378. https://doi.org/10.1016/j.gde.2009.06.001

Poethig RS (2013) Vegetative phase change and shoot maturation in plants, 1st edn. Elsevier Inc.

Pratt AJ, MacRae IJ (2009) The RNA-induced silencing complex: A versatile gene-silencing machine. J Biol Chem 284:17897–17901.

https://doi.org/10.1074/jbc.R900012200

Qian M, Ni J, Niu Q, Bai S, Bao L, Li J, Sun Y, Zhang D, Teng Y (2017) Response of miR156-SPL module during the red peel coloration of bagging-treated Chinese sand pear (*Pyrus pyrifolia* Nakai). Front Physiol 8:1–16. https://doi.org/10.3389/fphys.2017.00550

Qiu Z, Wang X, Gao J, Guo Y, Huang Z, Du Y (2016) The tomato Hoffman's anthocyaninless gene encodes a bHLH transcription factor involved in anthocyanin biosynthesis that is developmentally regulated and induced by low temperatures. PLoS One 11:1–22. https://doi.org/10.1371/journal.pone.0151067

Ramamoorthy S, Doss FP, Kundu K, Satyanarayana VSV, Kumar V (2010) Molecular characterization of bixin-An important industrial product. Ind Crops Prod 32:48–53. https://doi.org/10.1016/j.indcrop.2010.03.001

Reinhart BJ, Weinstein EG, Rhoades MW, Bartel B, Bartel DP (2002) MicroRNAs in plants. Trends Plant Sci 7:1616–1626. https://doi.org/10.1101/gad.1004402.of

Reis RS, Vale EM, Sousa KR, Santa-Catarina C, Silveira V (2021) Pretreatment free of 2,4-dichlorophenoxyacetic acid improves the differentiation of sugarcane somatic embryos by affecting the hormonal balance and the accumulation of reserves. Plant Cell Tissue Organ Cult 145:101–115. https://doi.org/10.1007/s11240-020-01995-z

Rivera-Madrid R, Burnell J, Aguilar-Espinosa M, Rodríguez-Ávila NL, Lugo-Cervantes E, Sáenz-Carbonell LA (2013) Control of Carotenoid Gene Expression in *Bixa orellana* L. Leaves Treated with Norflurazon. Plant Mol Biol Report 31:1422–1432. https://doi.org/10.1007/s11105-013-0604-1

Rose KME, Mickelbart M V., Jacobs DF (2019) Plasticity of phenotype and heteroblasty in contrasting populations of *Acacia koa*. Ann Bot 124:399–409. https://doi.org/10.1093/aob/mcz083

Rubinelli PM, Chuck G, Li X, Meilan R (2013) Constitutive expression of the Corngrass1 microRNA in poplar affects plant architecture and stem lignin content and composition. Biomass and Bioenergy 54:312–321. https://doi.org/10.1016/j.biombioe.2012.03.001

Salazar-Chavarría V, Sánchez-Nieto S, Cruz-Ortega R (2020) Fagopyrum esculentum at early stages copes with aluminum toxicity by increasing ABA levels and antioxidant system. Plant Physiol Biochem 152:170–176.

https://doi.org/10.1016/j.plaphy.2020.04.024

Santos DC dos, Silva Barboza A da, Ribeiro JS, Rodrigues Junior SA, Campos ÂD, Lund RG (2021) *Bixa orellana* L. (Achiote, Annatto) as an antimicrobial agent: A scoping review of its efficiency and technological prospecting. J Ethnopharmacol 287:114961. https://doi.org/10.1016/j.jep.2021.114961

Schäfer M, Brütting C, Meza-Canales ID, Großkinsky DK, Vankova R, Baldwin IT, Meldau S (2015) The role of cis-zeatin-type cytokinins in plant growth regulation and mediating responses to environmental interactions. J Exp Bot 66:4873–4884. https://doi.org/10.1093/jxb/erv214

Schneider CA, Rasband WS, Eliceiri KW (2012) NIH Image to ImageJ: 25 years of Image Analysis. Nat Methods 9:185–188. https://doi.org/10.1007/978-1-84882-087-6_9

Shimizu-Sato S, Tanaka M, Mori H (2009) Auxin-cytokinin interactions in the control of shoot branching. Plant Mol Biol 69:429–435. https://doi.org/10.1007/s11103-008-9416-3

Silva PO, Batista DiS, Cavalcanti JHF, Koehler AD, Vieira LM, Fernandes AM, Barrera-Rojas CH, Ribeiro DiM, Nogueira FTS, Otoni WC (2019) Leaf heteroblasty in Passiflora edulis as revealed by metabolic profiling and expression analyses of the microRNAs miR156 and miR172. Ann Bot 123:1191–1203. https://doi.org/10.1093/aob/mcz025

Singh A, Dwivedi P (2018) Methyl-jasmonate and salicylic acid as potent elicitors for secondary metabolite production in medicinal plants: A review. J Pharmacogn Phytochem 7:750–757

Su YH, Liu YB, Zhang XS (2011) Auxin-cytokinin interaction regulates meristem development. Mol Plant 4:616–625. https://doi.org/10.1093/mp/ssr007

THE ANGIOSPERM PHYLOGENY GROUP. An update of the Angiosperm Phylogeny Group classification for the orders and families of flowering plants: APG III. Bot J Linn Soc. 2009;161:105–21.2.

THE ANGIOSPERM PHYLOGENY GROUP. An update of the Angiosperm Phylogeny Group classification for the orders and families of flowering plants: APG II. Bot J Linn Soc. 2003;141:399–436.

Tonnessen BW, Manosalva P, Lang JM, Baraoidan M, Bordeos A, Mauleon R, Oard J, Hulbert S, Leung H, Leach JE (2015) Rice phenylalanine ammonia-lyase gene

OsPAL4 is associated with broad spectrum disease resistance. Plant Mol Biol 87:273–286. https://doi.org/10.1007/s11103-014-0275-9

Vaccaro M, Malafronte N, Alfieri M, De Tommasi N, Leone A (2014) Enhanced biosynthesis of bioactive abietane diterpenes by overexpressing AtDXS or AtDXR genes in *Salvia sclarea* hairy roots. Plant Cell Tissue Organ Cult 119:65–77. https://doi.org/10.1007/s11240-014-0514-4

Valério MA, Ramos MIL, Braga Neto JA, Macedo MLR (2015) Annatto seed residue (*Bixa orellana* L.): Nutritional quality. Food Sci Technol 35:326–330. https://doi.org/10.1590/1678-457X.6539

Vanstraelen M, Benková E (2012) Hormonal interactions in the regulation of plant development. Annu Rev Cell Dev Biol 28:463–487. https://doi.org/10.1146/annurev-cellbio-101011-155741

Varkonyi-Gasic E, Wu R, Wood M, Walton EF, Hellens RP (2007) Protocol: A highly sensitive RT-PCR method for detection and quantification of microRNAs. Plant Methods 3:1–12. https://doi.org/10.1186/1746-4811-3-12

Vilar DDA, Vilar MSDA, Moura TFADL, Raffin FN, Oliveira MR De, Franco CFDO, De Athayde-Filho PF, Diniz MDFFM, Barbosa-Filho JM (2014) Traditional Uses, chemical constituents, and biological activities of *Bixa orellana* L.: A review. Sci World J 2014:. https://doi.org/10.1155/2014/857292

Visentin I, Pagliarani C, Deva E, Caracci A, Turečková V, Novák O, Lovisolo C, Schubert A, Cardinale F (2020) A novel strigolactone-miR156 module controls stomatal behaviour during drought recovery. Plant Cell Environ 43:1613–1624. https://doi.org/10.1111/pce.13758

Wang G, Bronson KF, Thorp KR, Mon J, Badaruddin M (2014) Multiple leaf measurements improve effectiveness of chlorophyll meter for durum wheat nitrogen management. Crop Sci 54:817–826. https://doi.org/10.2135/cropsci2013.03.0160

Wang H, Wang H (2015) The miR156/SPL module, a regulatory hub and versatile toolbox, gears up crops for enhanced agronomic traits. Mol Plant 8:677–688. https://doi.org/10.1016/j.molp.2015.01.008

Wang J, Ye Y, Xu M, Feng L, Xu LA (2019a) Roles of the SPL gene family and miR156 in the salt stress responses of tamarisk (*Tamarix chinensis*). BMC Plant Biol 19:1–11. https://doi.org/10.1186/s12870-019-1977-6

Wang JW, Czech B, Weigel D (2009) miR156-Regulated SPL Transcription Factors Define an Endogenous Flowering Pathway in *Arabidopsis thaliana*. Cell 138:738–749. https://doi.org/10.1016/j.cell.2009.06.014

Wang L, Liu X, Wang X, Pan Z, Geng X, Chen B, Liu B, Du X, Song X (2019b) Identification and characterization analysis of sulfotransferases (SOTs) gene family in cotton (*Gossypium*) and its involvement in fiber development. BMC Plant Biol 19:1–13. https://doi.org/10.1186/s12870-019-2190-3

Wang L, Yu P, Lyu J, Hu Y, Han C, Bai MY, Fan M (2021) Bzr1 physically interacts with spl9 to regulate the vegetative phase change and cell elongation in arabidopsis. Int J Mol Sci 22:. https://doi.org/10.3390/ijms221910415

Wang M, Zhu X, Li Y, Xia Z (2020a) Transcriptome analysis of a new maize albino mutant reveals that zeta-carotene desaturase is involved in chloroplast development and retrograde signaling. Plant Physiol Biochem 156:407–419. https://doi.org/10.1016/j.plaphy.2020.09.025

Wang QL, Sun AZ, Chen ST, Chen LS, Guo FQ (2018) SPL6 represses signalling outputs of ER stress in control of panicle cell death in rice. Nat Plants 4:280–288. https://doi.org/10.1038/s41477-018-0131-z

Wang S, Chen Z, Tian L, Ding Y, Zhang J, Zhou J, Liu P, Chen Y, Wu L (2019c) Comparative proteomics combined with analyses of transgenic plants reveal ZmREM1.3 mediates maize resistance to southern corn rust. Plant Biotechnol J 17:2153–2168. https://doi.org/10.1111/pbi.13129

Wang S, Wu K, Yuan Q, Liu X, Liu Z, Lin X, Zeng R, Zhu H, Dong G, Qian Q, Zhang G, Fu X (2012) Control of grain size, shape and quality by OsSPL16 in rice. Nat Genet 44:950–954. https://doi.org/10.1038/ng.2327

Wang Y, Liu W, Wang X, Yang R, Wu Z, Wang H, Wang L, Hu Z (2020b) MiR156 regulates anthocyanin biosynthesis through SPL targets and other microRNAs in poplar. Hortic Res 7:1–12. https://doi.org/10.1038/s41438-020-00341-w

Wani AB, Chadar H, Wani AH, Singh S, Upadhyay N (2017) Salicylic acid to decrease plant stress. Environ Chem Lett 15:101–123. https://doi.org/10.1007/s10311-016-0584-0

Warren CR (2008) Rapid measurement of chlorophylls with a microplate reader. J Plant Nutr 31:1321–1332. https://doi.org/10.1080/01904160802135092

Wei S, Gruber MY, Yu B, Gao MJ, Khachatourians GG, Hegedus DD, Parkin IAP,

Hannoufa A (2012) Arabidopsis mutant sk156 reveals complex regulation of SPL15 in a miR156-controlled gene network. BMC Plant Biol 12:. https://doi.org/10.1186/1471-2229-12-169

Wellburn AR (1994) The Spectral Determination of Chlorophylls a and b, as well as Total Carotenoids, Using Various Solvents with Spectrophotometers of Different Resolution. J Plant Physiol 144:307–313. https://doi.org/10.1016/S0176-1617(11)81192-2

Wiśniewski JR, Zougman A, Nagaraj N, Mann M (2009) Universal sample preparation method for proteome analysis. Nat Methods 6:359–362. https://doi.org/10.1038/nmeth.1322

Wu G, Park MY, Conway SR, Wang J, Wigel D, Poethig RS (2009) The sequential action of miR156 and miR172 regulates developmental timing in Arabidopsis. Cell 6:1249–1254. https://doi.org/10.1016/j.cgh.2008.07.016.Cytokeratin

Wu G, Poethig RS (2006) Temporal regulation of shoot development in Arabidopsis thaliana by miRr156 and its target SPL3. Development 133:3539–3547. https://doi.org/10.1242/dev.02521

Wu Z, Cao Y, Yang R, Qi T, Hang Y, Lin H, Zhou G, Wang ZY, Fu C (2016) Switchgrass SBP-box transcription factors PvSPL1 and 2 function redundantly to initiate side tillers and affect biomass yield of energy crop. Biotechnol Biofuels 9:1–15. https://doi.org/10.1186/s13068-016-0516-z

Xie K, Shen J, Hou X, Yao J, Li X, Xiao J, Xiong L (2012) Gradual increase of miR156 regulates temporal expression changes of numerous genes during leaf development in rice. Plant Physiol 158:1382–1394. https://doi.org/10.1104/pp.111.190488

Xie Y, Liu Y, Wang H, Ma X, Wang B, Wu G, Wang H (2017) Phytochrome-interacting factors directly suppress MIR156 expression to enhance shade-avoidance syndrome in Arabidopsis. Nat Commun 8:. https://doi.org/10.1038/s41467-017-00404-y

Xing S, Salinas M, Höhmann S, Berndtgen R, Huijser P (2010) miR156-targeted and nontargeted SBP-Box transcription factors act in concert to secure male fertility in Arabidopsis. Plant Cell 22:3935–3950. https://doi.org/10.1105/tpc.110.079343

Yokota T (1997) The structure, biosynthesis and function of brassinosteriods. Trends Plant Sci 2:137–143. https://doi.org/10.1016/S1360-1385(97)01017-0

Yu N, Cai WJ, Wang S, Shan CM, Wang LJ, Chena XY (2010) Temporal control of trichome distribution by microRNA156-targeted SPL genes in *Arabidopsis thaliana*. Plant Cell 22:2322–2335. https://doi.org/10.1105/tpc.109.072579

Yu N, Niu QW, Ng KH, Chua NH (2015a) The role of miR156/SPLs modules in Arabidopsis lateral root development. Plant J 83:673–685. https://doi.org/10.1111/tpj.12919

Yu S, Galvão VC, Zhang YC, Horrer D, Zhang TQ, Hao YH, Feng YQ, Wang S, Schmid M, Wang JW (2012) Gibberellin regulates the Arabidopsis floral transition through miR156-targeted SQUAMOSA PROMOTER BINDING-LIKE transcription factors. Plant Cell 24:3320–3332. https://doi.org/10.1105/tpc.112.101014

Yu X, Zhang W, Zhang Y, Zhang X, Lang D, Zhang X (2019) The roles of methyl jasmonate to stress in plants. Funct Plant Biol 46:197–212. https://doi.org/10.1071/FP18106

Yu ZX, Wang LJ, Zhao B, Shan CM, Zhang YH, Chen DF, Chen XY (2015b) Progressive regulation of sesquiterpene biosynthesis in arabidopsis and patchouli (*Pogostemon cablin*) by the MIR156-targeted SPL transcription factors. Mol Plant 8:98–110. https://doi.org/10.1016/j.molp.2014.11.002

Zarei A, Trobacher CP, Shelp BJ (2016) Arabidopsis aldehyde dehydrogenase 10 family members confer salt tolerance through putrescine-derived 4-aminobutyrate (GABA) production. Sci Rep 6:. https://doi.org/10.1038/srep35115

Zhang B, You C, Zhang Y, Zeng L, Hu J, Zhao M, Chen X (2020) Linking key steps of microRNA biogenesis by TREX-2 and the nuclear pore complex in Arabidopsis. Nat Plants 6:957–969. https://doi.org/10.1038/s41477-020-0726-z

Zhang TQ, Wang JW, Zhou CM (2015) The role of miR156 in developmental transitions in *Nicotiana tabacum*. Sci China Life Sci 58:253–260. https://doi.org/10.1007/s11427-015-4808-5

Zhang X, Liu CJ (2015) Multifaceted regulations of gateway enzyme phenylalanine ammonia-lyase in the biosynthesis of phenylpropanoids. Mol Plant 8:17–27. https://doi.org/10.1016/j.molp.2014.11.001

Zhang Y, Yang J, Lu S, Cai J, Guo Z (2008) Overexpressing SgNCED1 in tobacco increases ABA level, antioxidant enzyme activities, and stress tolerance. J Plant Growth Regul 27:151–158. https://doi.org/10.1007/s00344-008-9041-z

Zheng C, Ye M, Sang M, Wu R (2019) A regulatory network for mir156-spl module in

Arabidopsis thaliana. Int J Mol Sci 20:. https://doi.org/10.3390/ijms20246166

Zhou Q, Shi J, Li Z, Zhang S, Zhang S, Zhang J, Bao M, Liu G (2021) MiR156/157 Targets SPLs to Regulate Flowering Transition, Plant Architecture and Flower Organ Size in Petunia. Plant Cell Physiol 62:839–857. https://doi.org/10.1093/pcp/pcab041

Zhou Y, Zhou B, Pache L, Chang M, Khodabakhshi AH, Tanaseichuk O, Benner C, Chanda SK (2019) Metascape provides a biologist-oriented resource for the analysis of systems-level datasets. Nat Commun 10:. https://doi.org/10.1038/s41467-019-09234-6

Zhu LS, Liang SM, Chen LL, Wu CJ, Wei W, Shan W, Chen JY, Lu WJ, Su XG, Kuang JF (2020) Banana MaSPL16 Modulates Carotenoid Biosynthesis during Fruit Ripening through Activating the Transcription of Lycopene β-Cyclase Genes. J Agric Food Chem 68:1286–1296. https://doi.org/10.1021/acs.jafc.9b07134

Zhu QH, Upadhyaya NM, Gubler F, Helliwell CA (2009) Over-expression of miR172 causes loss of spikelet determinacy and floral organ abnormalities in rice (*Oryza sativa*). BMC Plant Biol 9:. https://doi.org/10.1186/1471-2229-9-149